IEEE Photonics Journal
An IEEE Photonics Society Publication

Recent Advances in Silica Glass Optical Fiber for Dosimetry Applications

Volume 12, Number 3, June 2020

H.T. Zubair
Mahfuza Begum
Farhad Moradi
A.K.M. Mizanur Rahman
Ghafour A. Mahdiraji
Adebiyi Oresegun
G.T. Louay
Nasr Y.M. Omar
Mayeen U. Khandaker
Faisal R. M. Adikan
Noramaliza M. Noor
K.S. Almugren
Hairul Azhar Abdul-Rashid
David A. Bradley

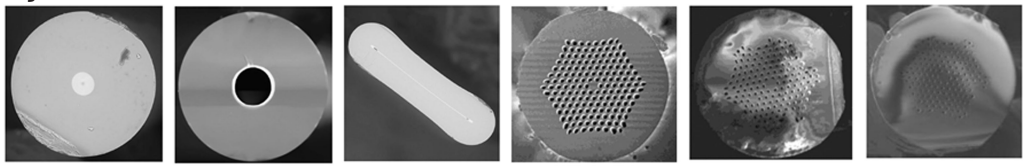

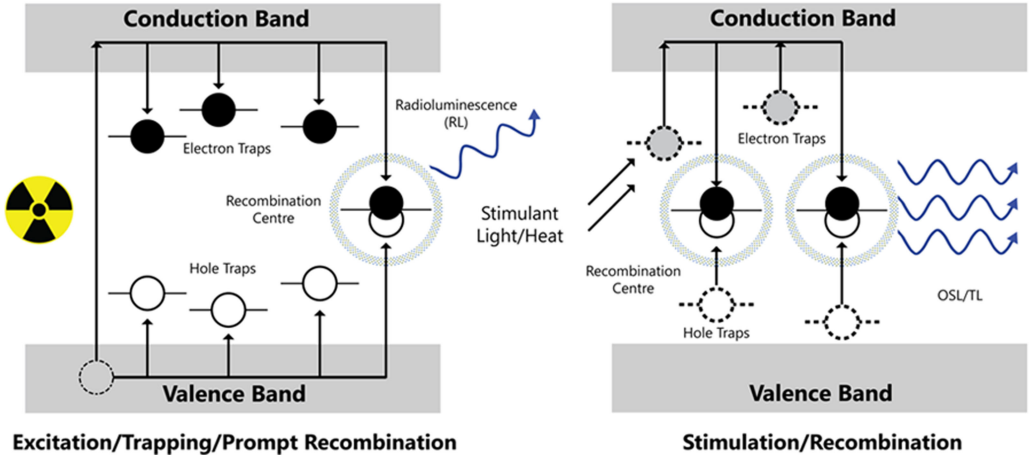

DOI: 10.1109/JPHOT.2020.2985857

Recent Advances in Silica Glass Optical Fiber for Dosimetry Applications

H.T. Zubair,[1] **Mahfuza Begum**,[2] **Farhad Moradi**,[3] **A.K.M. Mizanur Rahman**,[4] **Ghafour A. Mahdiraji**,[5] **Adebiyi Oresegun**,[1] **G.T. Louay**,[1] **Nasr Y.M. Omar**,[1] **Mayeen U. Khandaker**,[6] **Faisal R. M. Adikan**,[7] **Noramaliza M. Noor**,[8] **K.S. Almugren**,[9] **Hairul Azhar Abdul-Rashid**,[1] **and David A. Bradley**[6]

[1]Fiber Optics Research Center, Faculty of Engineering, Multimedia University, Cyberjaya 63100, Malaysia
[2]Health Physics & Radioactive Waste Management Unit, Institute of Nuclear Science and Technology, Atomic Energy Research Establishment, Bangladesh Atomic Energy Commission, Ganakbari, Savar, Dhaka, Bangladesh
[3]Department of Physics, University of Malaya, Kuala Lumpur, Malaysia
[4]Health Physics Division Atomic Energy Centre, Bangladesh Atomic Energy Commission, Shahbag 1000, Bangladesh
[5]Dura-Mine Sdn. Bhd., Branang, Selangor 43700, Malaysia; Flexilicate Sdn. Bhd., University of Malaya, Kuala Lumpur 50603, Malaysia
[6]Center for Biomedical Physics, School of Healthcare and Medical Sciences, Sunway University, Bandar Sunway 47500, Malaysia
[7]Integrated Lightwave Research Group, Department of Electrical Engineering, Faculty of Engineering, , University of Malaya, Kuala Lumpur 50603, Malaysia
[8]Department of Imaging Faculty of Medicine and Health Sciences, Universiti Putra Malaysia, Serdang 40100, Malaysia
[9]Dept. of Physics, Princess Nourah Bint Abdulrahman University, Riyadh, Saudi Arabia; Department of Physics, University of Surrey, Guildford GU2 7XH, U.K.

DOI:10.1109/JPHOT.2020.2985857

Manuscript received February 14, 2020; revised March 23, 2020; accepted March 31, 2020. Date of publication April 10, 2020; date of current version May 12, 2020. Corresponding author: Hairul Azhar Abdul-Rashid (e-mail: hairul@mmu.edu.my).

Abstract: In this paper, we review the highly promising silica glass, fabricated as doped and undoped optical fiber for intended use in radiation dosimetry. The dosimetry techniques reviewed here, underpinned by intrinsic and extrinsic defects in silica glass, focus on Thermoluminescence (TL), Optically Stimulated Luminescence (OSL) and Radioluminescence (RL), with occasional references to the much more established Radiation Induced Attenuation (RIA). The other focus in this review is on the various materials that have been reported earlier as dopants and modifiers used in silica glass optical fiber radiation dosimeters. This article also elaborates on recently reported optical fiber structures, namely, cylindrical fibers, photonic crystal fibers and flat fibers, as well as dimensions and shapes used for optimization of dosimeter performance. The various types of optical fiber radiation dosimeters are subsequently reviewed for various applications ranging from medical dosimetry such as in external beam radiotherapy, brachytherapy and diagnostic imaging, as well as in industrial processing and space dosimetry covering a dynamic dose range from μGy to kGy. Investigated dosimetric characteristics include reproducibility, fading, dose response, reciprocity between luminescence yield to dose-rate and energy dependence. The review is completed by a brief discussion on limitations and future developments in optical fiber radiation dosimetry.

Index Terms: Silica optical fiber, dosimetry, radioluminescence, thermoluminescence, review.

1. Introduction

Ionizing radiation has many applications ranging from industrial and food processing to medical treatment and diagnostics. In order to ensure effective and consistent delivery of ionizing radiation to achieve the intended purpose in such applications, radiation monitoring and dosimetry is a very important aspect. Different approaches to radiation dosimetry have been reported ranging from passive methods such as thermoluminescence (TL) and active methods using diodes, ion chambers and scintillators.

Advances in the delivery of external therapeutic beams in radiotherapy continue to drive demands on dosimetric systems, for both point-dose and dose distribution evaluations. Challenges include obtaining a linear response across the large dynamic range of dose and dose-rates. The spatial resolution and accuracy required of a dosimeter to measure the radiotherapy dose distribution of such complex 3D geometries is becoming more challenging. Current commercially available field dosimeters are not suitable in such challenging situations owing to their relatively large dimensions. This has been true for both active and passive dosimeters.

Silica glass optical fiber has emerged as one of the candidates to fill in the gap, especially in the aspect of spatial resolution (sub-mm), accuracy and large dynamic range. Originally designed for optical communications, such optical fibers are typically doped with germanium to provide total internal reflection required for communication purposes. Studies of potential radiation therapy applications of the optical fiber started with TL passive dosimeters, undertaken by several groups. Some of the different aspects studied include TL passive dosimetry [1]–[3], radiation induced attenuation (RIA) [4], radioluminescence (RL) and optically stimulated luminescence (OSL) [5]–[7]. Useful TL emission has been observed at the radiation levels familiarly applied in high dose radiation-medicine procedures.

Besides the general characteristics of optical fiber radiation dosimeters such as cost effectiveness, sufficient sensitivity [8], acceptable fading [9], response linearity and reproducibility [10] and dose rate independence [11], they have some unique properties providing for the possibility of precision measurement of dose in tissues. These include water-resistance and spatial resolution of down to 100 μm. Current increasing interest in advanced radiotherapy techniques is toward the utilization of small radiation fields as well as high dose rate treatments that usually result in a high dose area with steep dose-rate drop off margins. Examples of such treatment modalities are intensity modulated radiation therapy (IMRT), volumetric modulated arc therapy (VMAT) and high dose rate radionuclide or electronic brachytherapy. Such therapy techniques allow for highly conformal target irradiation that boost the tumor dose and results in better treatment outcome, however they also raise the need for patient to patient in vivo dosimetry for verification of correct dose delivery. Spatial resolution of the dosimeter is a key characteristic in such situations in order to reduce any volume averaging effect and also to avoid perturbing the radiation field [12], [13].

Herein, we detail efforts by various groups in utilizing the highly promising silica glass, in the form of doped and undoped optical fiber, as radiation dosimeters, based on RIA, TL, OSL and RL. The applications have been categorized as medical and non-medical since a large volume of work in the recent past has focused on therapeutic and diagnostic radiation environments.

In the next section, the techniques utilized by fiber optic-based dosimetry systems are briefly described. This is followed by a section focusing on the MCVD fabrication technique (the techniques used by a large proportion of studies in this review), the different structures of optical fibers produced for dosimetric applications, the commonly used dopants, the dimensions and geometry, and the effective atomic number of silica based optical fibers. In section 4 and 5, the reported dose response characteristics in medical and non-medical applications are discussed, followed by a discussion on the limitations of optical fibers in dosimetric applications.

2. Techniques

The underpinning phenomenon for all the aforementioned techniques are intrinsic defects and the electron-hole pairs generated by the ionizing radiation, subsequently being trapped at defect sites,

giving rise to optical absorption and luminescence [14]. Intrinsic defects are present in the matrix of a pure Silica glass optical fiber such as peroxy linkages (POL) and oxygen deficient centers (ODC). In disrupted SiO_2 tetrahedra the absence of oxygen or silicon atoms creates oxygen deficient and silicon deficient defects. POL (oxygen interstitials) and ODC (oxygen deficient centers) familiarly designated E′, when exposed to ionizing radiation trap holes to form peroxy radicals (POR) and E' centers respectively. In rapidly cooled silica, strained Si-O-Si bonds are cut when exposed to ionizing radiation to form non-bridging oxygen hole centers (NBOHC) and E' centers by trapping holes and electrons, respectively [15], [16].

2.1 Radiation Induced Attenuation

When silica glass optical fibers are exposed to ionizing radiation, a form of 'damage' occurs in the optical fiber, leading to additional attenuation of the propagating optical signal [17]. This leads to decreased power at the output end. Since the radiation induced attenuation (RIA) of certain wavelengths/bands has been found to be linear with the absorbed dose, given a particular composition of the optical fiber, it is a potential mechanism for dosimetry.

The attenuation or 'darkening' occurs due to chemical bonds in the optical fiber core that are disrupted by the ionizing radiation. Exposure to such high energy ionizing radiation results in new electronic transition states or defects leading to additional absorption at specific wavelengths. When the ionizing radiation is removed, the optical fiber recovers to its original state with some remaining 'damage'. The severity of such damage is influenced by defect generation (attenuation) and annihilation (recovery) [18].

Greater RIA occurs in doped silica glass and leads to better dosimetry measurements. To improve the radiation dosimetry performance, it is necessary to increase the density of such intrinsic defects. This can be achieved by incorporating impurities in silica glass (such as germanium, phosphorus and aluminium), controlling the input gas composition, optimizing the thermal treatment at all stages of fiber manufacturing and optimizing the stress in the optical fiber core [19].

Typical optical fibers undergo darkening which depends on ionization type, optical fiber core glass composition, operating wavelength, dose rate, total accumulated dose, temperature and power propagating through the optical fiber core. The presence of dopants in the optical fiber core (such as germanium, phosphorus, boron, aluminum, erbium, ytterbium, thulium and holmium) increases the RIA [20].

[21] reported three single-mode fibers drawn from MCVD-made pure-silica-core F-doped-silica-cladding preform. The drawing parameters such as temperature, speed, and tension were varied. RIA was observed to increase with increased drawing temperature. The RIA was however found to increase less with increased speed and tension. This strong drawing temperature effect on RIA has been associated with concentration of strain-assisted radiation-induced self-trapped holes.

2.2 Thermoluminescence and Optically Stimulated Luminescence

In the thermoluminescence dosimetry method, thermally stimulated light is emitted from an insulator or semiconductor due to absorption of energy from ionizing radiation. The fundamental principles in TL relate to the impurities in the TL material that creates localized energy levels within the forbidden energy band gap [22]. A simple energy band model for thermoluminescence process [23] is represented in Fig. 1.

In TL materials, when ionizing radiation is absorbed, free electrons and holes are generated. Electrons are excited from the valence band to the conduction band. These electrons may be trapped in the material owing to lattice defects or impurities. Free positive holes also travel through the valence band and may become trapped. Many hole centers are thermally unstable and can decay quickly at normal room temperature [23]. The trapped electrons persist in their traps until they attain adequate energy to escape. Before saturation happens, there is a direct relation between the amount of trapped electrons and applied radiation dose [2].

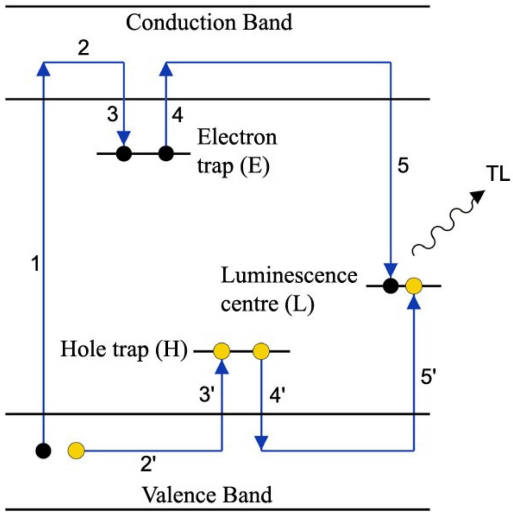

Fig. 1. Simple energy band model for TL process [23].

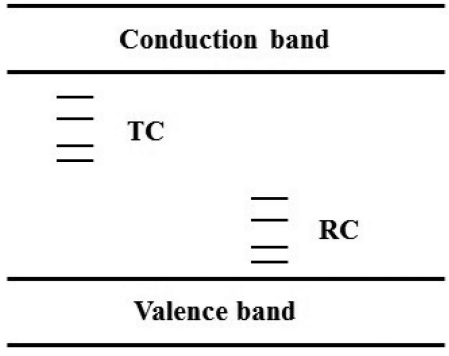

Fig. 2. Schematic diagram of TL model with multi-level trapping and recombination centers. TC and RC refer to trapping center and recombination center respectively.

By heating the material, these “trapped electrons” escape and recombine with holes at luminescence centers. Consequently, light is emitted with intensity directly related to the radiation dose absorbed by the material (IAEA Safety Standard Series, 1999).

In addition to the process shown in Fig. 1, recombination may also take place in electron centers or even the valence band. Not all of the possible recombination events are radiative, resulting in photon emission. The model described with two energy levels is the simplest model that can be used to explain thermoluminescence but obviously is not sufficient to describe thermoluminescence from a real TL material at least because it cannot predict the presence of the several TL peaks in the material glow curve observed in the most popular TLDs, an instance being LiF with four glow peaks. Experimental observations have suggested the existence of a range of trapping and recombination [24], [25] as can be seen schematically in Fig. 2 above. There are two possible scenarios arising from the presence of a collection of traps:(i) electrons from different trap levels form a single recombination center; (ii) electrons from the same trap depth create several recombination centers. Luminescence of differing wavelength will accordingly manifest as distinct TL peaks [26].

Broad glow curves observed from polycrystalline or amorphous materials like Silica that do not show distinct TL peaks, are in agreement with expectations from such a multi-trap and recombination centers model. [27] had suggested a band gap model including a thermally disconnected trap (TDT) much deeper than normal traps that can be filled during the irradiation stage but not releasing

electrons during the heating stage like normal (shallow) traps. Incorporation of TDT helps provide justification of wide glow peaks of amorphous silica and other experimental observations from such materials. In general, theoretical studies have been made and are still in process introducing more complex models to explain characteristics observed from various TL materials.

For the case of OSL, use is made of light of appropriate wavelength (having the necessary energy to release trapped electrons) instead of heat. The use of light enables simpler readout setup, and is faster because of the absence of a heating/cooling process and the possibility of applying light to released trapped charge carriers simultaneously or immediately after irradiation.

The TL properties of silica fiber depend on the trapping process that is caused by the occurrence of structural defects in the material [28]. Dosimetric characteristics of fiber dosimeter have pointed to the considerable potential for use with megavoltage X-ray beams [1], [29], electron beams [30], [31], proton beams [32], alpha particles [33], fast neutrons [34] and gamma rays [3], [35], [36]. Commercial Ge-doped silica fibers have also been used to measure photo-electron dose enhancement from iodinated contrast media, with potential interest with respect to the radiation synovectomy technique [28].

2.3 Radioluminescence

Radioluminescence is generated by free charge (electrons and holes induced by ionizing radiation) recombining at color centers. The wavelength of RL is often identical to fluorescence, but the lifetime may extend into milliseconds.

Regardless of the initial energy transfer mechanism (depending on the initial photon energy usually dominated by Compton scattering and photoelectric absorption or in the case of charged particles dominated by Coulomb interactions), energy from the ionizing radiation is dispersed in the scintillator material by delta rays or secondary electrons. The secondary electrons cause further excitation and ionization in the material, and the process continues until there is insufficient energy for further ionization. This results in the formation of large number of electrons and holes. These electrons further lose energy by interaction with crystal vibrations in electron-phonon relaxation or thermalization. During this process, the electrons migrate to the bottom of the conduction band, and the holes travel towards the top of the valence band. This process occurs in a timescale of the order of 10^{-11} to 10^{-12} s. This arrangement allows the electron-hole pairs to recombine in different processes. In materials with large number of defects, the electron is captured in a trap, where it recombines with a hole, or vice versa. This recombination is radiative and constitutes RL [37].

A simplified model of the conversion of ionization radiation energy into visible light is illustrated in Fig. 3. Take, for example, the NaI crystal. Pure NaI has a bandgap of 5.9 eV. When ionizing radiation interacts with this crystal, the energy from one photon of the beam is transferred to one electron in the crystal. If this electron were to travel to the conduction band (CB) and return to the valence band (VB) by radiative relaxation, the resultant photon would have a wavelength of around 210 nm. This photon belongs to deep UV region, and will soon interact with other electrons in the crystal to dissipate the energy, resulting in no photon energy leaving the crystal. The addition of a small amount of activator such as Thallium (Tl), helps create intermediate energy bands between the CB and VB. Now, as the excited electrons make their way down to the VB, they drop in small steps (losing small energy every time) into exciton states eventually emitting a photon of a lower energy and longer wavelength (visible) that can leave the crystal.

3. Materials, Fabrication and Structures

3.1 Fabrication

The optical fibers for dosimetry are primarily fabricated using the MCVD technique, produced in a high temperature environment using $GeCl_4$ and $SiCl_4$ as the precursor [38], [39]. Besides MCVD, methods such as extrusion [40], [41] and sol-gel [42] have been reported, but these are beyond the scope of this review paper. A schematic of an MCVD system is illustrated in Fig. 4. An MCVD

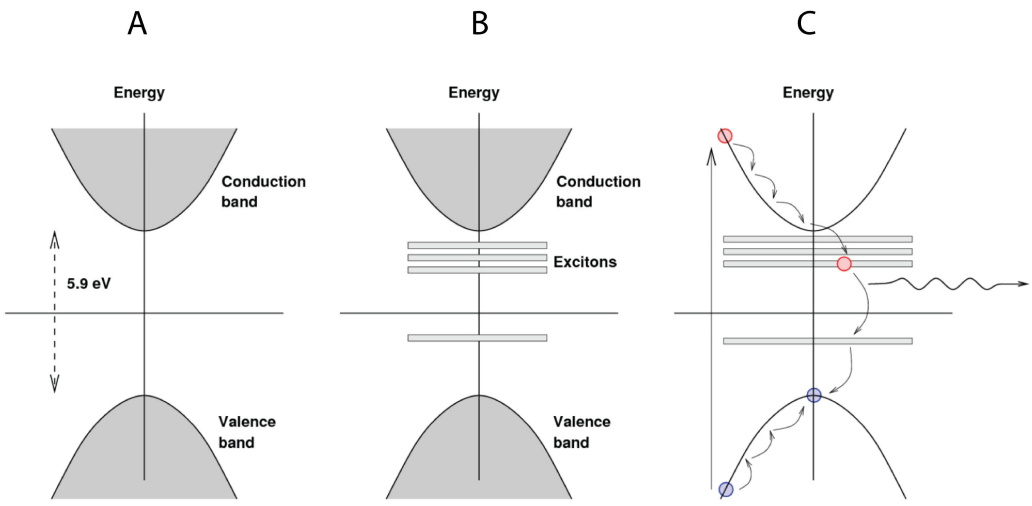

Fig. 3. Formation of new bands between CB and VB to accommodate excitons by addition of dopants.

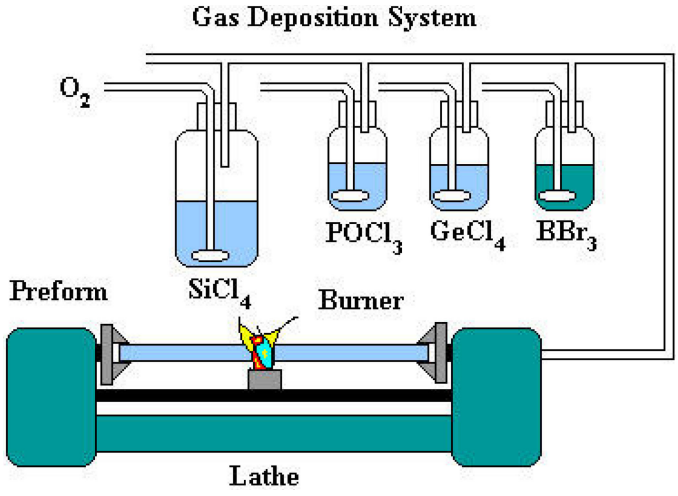

Fig. 4. A schematic diagram of an MCVD system (Freudenrich, 2001).

system is comprised of two major components: the gas and material delivery system and the lathe. The gas deposition system is a delivery system used to transport the glass-forming reagent to the reaction zone. Typical glass-forming reagents used in the MCVD system are $SiCl_4$, $GeCl_4$, $POCl_3$, and BBr_3. These materials have a high saturated vapor pressure, which makes them suitable for mass transportation. These reagents are placed in a container called a "bubbler", which allows the carrier gas (i.e., O_2) to enter the container and carry the vapor form of the reagent to the deposition zone. Additionally, several other inert gases are included to assist either deposition (e.g., He) or dehydration (e.g., Cl_2) processes. On the lathe, a high-purity silica substrate tube is placed and heated to the reaction temperature using an oxy-hydrogen burner. The lathe rotates the substrate tube to ensure a radial uniformity of the deposited layer to be obtained at the inner wall of the tube. The burner moves transversely along the tube's longitudinal axis to allow the deposition to take place along its length.

The solution-doping technique is widely known as a reliable technique for doping rare earth elements inside high-purity silica. Unlike glass-forming materials, most glass modifiers including rare earths do not have precursor materials that exist in a liquid phase at room temperature. In

order to dope these materials inside silica, the solution-doping technique was first introduced by [43]. The method uses a porous layer of deposited silica soot as the absorbent for the rare earth or modifier salt solutions. These solutions impregnate the soot and upon drying, the rare earth or modifier salt remains on the surface or inside the voids of the soot. With proper heating and O_2 gas flow the salt is then converted to the corresponding oxide. However, the amount of dopant introduced by the solution-doping technique can be inconsistent from one preform to another due to the unclear relationship between the nature of the porous soot and the amount of salt that remains after soaking. Hence, the optimization of the solution-doping process has been the subject of numerous studies [44]–[48].

Developments beyond the commercially available telecommunication fiber, also obtained using the MCVD technique, have included fabrication of hollow cylindrical fibers, collapsed fibers, photonic crystal fibers and flat fibers, with various Ge dopant concentrations extrinsically introduced and with various dimensions. For instance, [49] have investigated three types of Ge-doped optical fibers: conventional cylindrical fiber, capillary fiber, and flat fiber (FF), all fabricated using the same optical fiber preform, shown in Fig. 11. For electron and photon irradiated fibers at doses from 0.5 to 8 Gy, the results show for capillary fiber collapsed into a flat shape that the TL yield is increased by 5.5, also some 3.2 times that of the cylindrical fiber. This suggests a strain-induced suitably sensitive TLD for in-vivo dosimeter applications, with changes in the glow curve also being observed. [50] have also shown that the sensitivity of FF constructs can be made to be competitive with phosphor-based TLD. Further investigations have concentrated on novel micro-structured fibers, one example being the photonic crystal fiber (PCF), produced by the stack and draw method, the TL arising from the dopant and induced strain [51].

3.2 Structures

In recent years, several reports discussed the influence of fiber structure on performance of fiber dosimeters. [52] compared the performance of capillary fibers made of three different materials, i.e., F300, Ge- and Ge-B-doped, with their collapsed version called flat fiber (FF). They have shown that by collapsing the capillary fiber into FF, thermoluminescence (TL) sensitivity of the fiber increased by 3, 12 and 31 times using the F300, Ge-doped, and Ge-B-doped fibers, respectively. The results suggest that by collapsing and fusing the surface walls of the capillaries, strain-related defects are created, increasing the TL yield many times over, and even more so if there is impurity/dopant in the collapsing surface area. [51] compared the performance of an un-doped single capillary with an un-doped photonic crystal fiber (PCF) that was made of 168 capillaries fabricated in the conventional stack-and-draw method. It is shown that the TL response of a single capillary is improved by 17.5 times after stack-and-drawing in PCF form. This performance is even further improved up to about 29.3 times when all the holes in the PCF are collapsed during the fiber drawing process. [49] compared the performance of a Ge-doped capillary fiber with a cylindrical fiber that was collapsed conventionally during the MCVD process and a FF that was collapsed during the fiber drawing. They have shown that the TL yield of the Ge-doped capillary is increased by a factor of 3.2 times by conventional collapsing into cylindrical form and 5.5 times by collapsing into flat shape all fabricated from the same preform. Table 1 and Table 2 shows the minimum detectable dose achieved by cylindrical and flat fibers pulled into the different structures from the same preform.

3.3 Materials

Several materials such as germanium [10], [53]–[57], boron [52], [58], aluminum [54], [59], [60], phosphorus [61], and thulium [60], [62] have been proposed for radiation dosimetry for different applications. Modified chemical vapor deposition (MCVD) is one of the common methods for doping such materials in silica fibers.

As will be seen in the following sections, germanium doped fiber is the one that has been most reported upon over the past decade specifically for medical applications, including *in vivo* dosimetry. One of the reasons why Ge-doped fibers have been used in the majority of the research work is

TABLE 1
A Summary of the Results of Minimum Detectable Dose (Cylindrical Fibers) [76]

Ge Dopant Concentrations (mol%)	Outer Diameters of Cylindrical Fibres (μm)	Minimum Detectable Dose (mGy)
6	241	~126
	604	~27
8	241	~188
	604	~58
10	241	~203
	604	~61

TABLE 2
A Summary of the Results of Threshold Dose (Flat Fibers) [50]

Ge-doped Flat Fiber Dimension (μm^2)	Threshold Dose (mGy)	
	Photon	Electron
60 X 180	4.07	3.91
100 X 350	3.68	3.46
200 X 750	3.50	3.10

because most of the standard telecommunication optical fibers are made of this material, having been established to be a cost-effective manufacturing process. Additionally, in terms of sensitivity, Ge-doped fibers have relatively high radiation sensitivity.

[52] compared the performance of suprasil F300, Ge-doped and Ge-boron (Ge-B) doped fibers. The latter showed superior radiation sensitivity compared to Ge-doped and F300. Ge-B-doped fiber has the advantage of lower effective atomic number, being closer to human tissue, thereby having less energy dependency compared to that of Ge-doped. This material would be a more suitable material for medical applications compared to Ge-doped. However, due to high fabrication costs due to boron doping and less accessibility of such fibers, there are a limited number of reports on this material.

[60] tested 13 types of fibers, differing in dopant, dopant concentration and diameter including P-, Al-, Er-, Ge- and Al-Tm-doped fibers, ultra-high numerical aperture (UH-NA) and borosilicate fiber, and two non-doped fibers including quartz and suprasil F300 glasses for the purpose of high-dose applications for electron and photon irradiations. They have shown that the ultra-high numerical aperture (UH-NA), Al-doped (4mol%), Er-doped, F300, Al-Tm-doped and Al-doped (2mol%) began to saturate in response at 40, 60, 60, 60, 60, and 80 kGy, respectively. However, borosilicate capillary shows the greatest potential for high dose application as it does not show any tendency towards saturation up to the tested dose of 100 kGy and a fading rate of 5-6% within the first 24 h and 11-12% after one week.

3.4 Dimensions

[63] investigated the influence of optical fiber diameter on TL response using optical fibers with either a fixed core-to-cladding ratio or different core-to-cladding ratios. They have shown that the TL signal of a Ge-doped fiber remained constant before and after removing part of the fiber cladding using HF acid. This suggests that the main TL signal is generated from the fiber Ge-doped core, while the cladding produces insignificant TL signal. On the other hand, the performance of five different diameters of optical fibers with the same core-to-cladding ratio have been compared using two different fiber preforms and reconfirmed with an un-doped silica rod. It is shown that

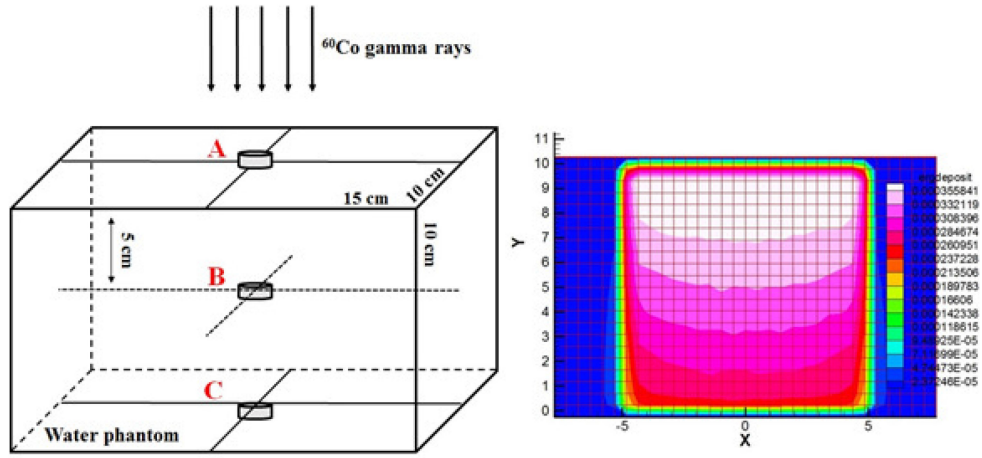

Fig. 5. Left hand: Schematic of the Monte Carlo simulation setup and position of the disk shape TLD. A) on entrance surface B) in the middle of the phantom and C) on the exit surface (in the case of rod shape TLD, it is horizontally positioned at the location of the disk), Right hand: Dose distribution in water phantom without dosimeter (Phantom is extended from X = −7.5 to X = 7.5 cm and from Y = 0 to Y = 10 cm).

the TL signal quadrupled when the fiber diameter is doubled before normalization. However, after normalization to their mass or cross-sectional area, they have shown that the greater sensitivity is observed from the fibers of smaller diameter compared to the fibers of larger diameter. This is suggested to be due to the shearing effect in the preform neck-down region where a smaller diameter fiber experiences greater shearing in the neck-down region compared to the larger diameter fiber, thereby inducing higher defects production in the fiber.

3.4.1 Dimensional Advantages of Optical Fibres for Medical Dosimetry: In order to evaluate perturbation produced in the radiation field caused by the presence of a silica fiber dosimeter and to compare it with that of a popular dosimeter, an irradiation set up was simulated. MCNPX Monte Carlo code (Los Alamos National Laboratory, USA) was used in simulation of a 15 $\times$ 10 $\times$ 10cm^3 water phantom and a Cobalt-60 source (with two gamma line energies of 1.1732 and 1.3325 MeV) generating a parallel beam exposing the phantom surface with 10 $\times$ 10 cm^2 field size. The most routinely used TLD material is lithium fluoride (LiF) with a density of 2.45 g/cm^3 (the average density of commercial materials ranged from 2.3 to 2.6 g/cm3) in disk shape with 2 mm diameter and 1 mm height. Disk dimensions are abbreviated here as (D, H) where D and H represent disk diameter and height. In addition to the same disk size made from silica, three sizes of rod shape silica TLDs with diameters of 500, 250 and 125 μm all with 3 mm length and measured density of 2.15 g/cm^3 were also considered. These are the usual size of silica optical fibers used in recent in vivo dosimetry studies [11], [64]. In three different set of models, TLDs were positioned at three different situations namely entrance phantom surface (A), middle of the phantom (B) and exit phantom surface (C) as schematically shown in Fig. 5-left hand. These positions were selected to cover both situations with and without establishment of charged particle equilibrium (CPE). The whole volume of the water phantom was voxelized with the cubic mesh size of 5 $\times$ 5 $\times$ 5 mm^3 (as shown in Fig. 5-right hand) while small mesh size of 1 $\times$ 1 $\times$ 1 mm^3 was used in order to calculate energy deposition in and around the dosimeter. Results of simulations for different shape and size dosimeters (in a 2D view on central plane) are shown in Figs. 6, 7 and 8 for situations A, B and C, respectively.

The upper and lower surface of the phantom are located at Y = 10 and Y = 0 positions in Figs. 6 and 8 where locations of disk or rod shape dosimeters are shown with dashed rectangles. Fig. 6 part A1 shows energy deposition on the surface of the water phantom where no dosimeter is existent. As expected from a Cobalt beam, deposited energy increases with depth in water as it reaches to its maximum at around 5 mm depth. It is evident from Fig. 6 that silica with the density

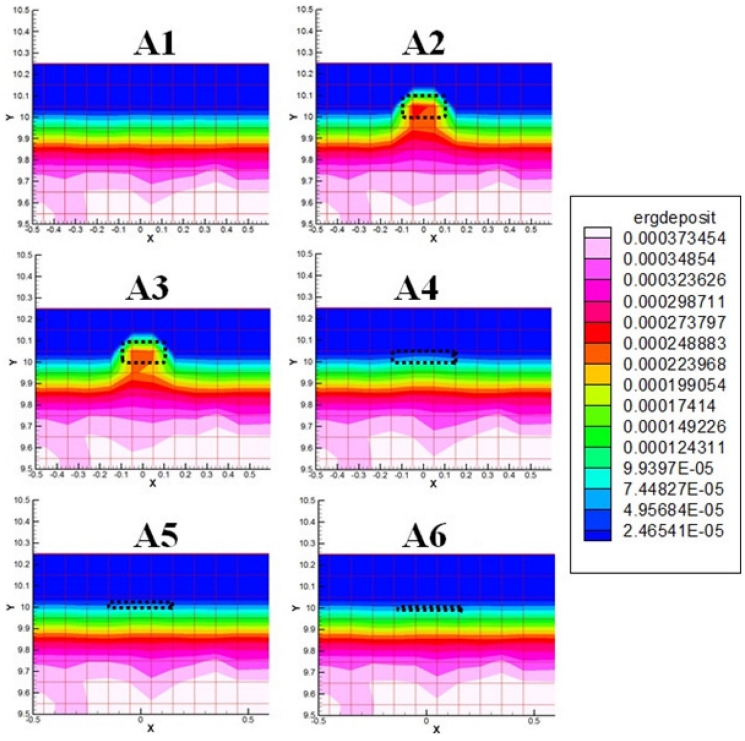

Fig. 6. Perturbation effect of various dosimeters positioned on water phantom entrance surface exposed by a ^{60}Co photon beam A1) water surface with no dosimeter, A2) LiF disk (2,1), A3) Silica (2,1), A4) Silica rod (0.5,3), A5) Silica rod (0.25,3), and A6) Silica rod (0.125,3).

of 2.15 g/cm^3 (A3) produces a comparable or even smaller perturbation compared to LiF with the density of 2.45 g/cm^3 (A2). This reveals the fact that, concerning dosimeter perturbation effect, density plays a more important role compared to the atomic number of the dosimeter compositional elements which is in agreement with the conclusions of a comprehensive study by [13]. Rod shape silica fibers with diameters of 500 μm (A4), 250 μm (A5) and 125 μm (A6) produce negligible perturbation compared to disk shape millimeter size TLDs where the effect decreases with fiber diameter. A similar pattern is observed at 5 mm depth in water where CPE is achieved (Fig. 7) and at the exit phantom surface where there is a high dose gradient (Fig. 8) supporting the same conclusion. This observation suggests that with an accurate calibration and identification of other sources of error in the process of luminescence measurement, sub-millimeter size silica fiber dosimeters with minimum perturbation compared to classical solid state dosimeters can provide superior precision measurements in specific situations of high dose gradients and small radiation fields.

3.5 Effective Atomic Number

[65] record it to be conventional to seek a Z_{eff} value that is ideally human soft-tissue equivalent (i.e., typically taken to be 7.42), with [66] going on to record that a Z_{eff} value that is human tissue equivalent is dependent on the incident photon energy and its direct association with the degree (the probability) to which primary photon interactions take place within the detector medium. With tissue equivalency playing a critical role in radiation therapy dosimetry, it is notable for instance that the photoelectric interaction is approximately proportional to the 3rd power of the material atomic number (Z^3). Tabulated in Table 3, [66] found that the Z_{eff} values (13.25–13.43) of the five optical fibers fall within the human-bones range of from 11.6 to 13.8, in keeping with [67], who also found

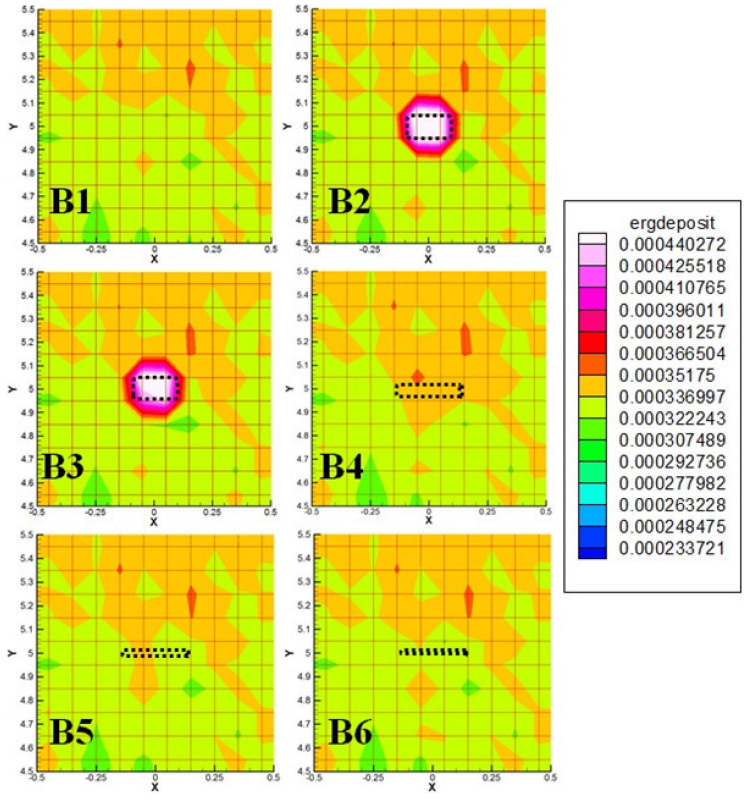

Fig. 7. Perturbation effect of various dosimeters positioned at 5 cm depth in water phantom exposed by a ^{60}Co photon beam B1) water with no dosimeter, B2) LiF disk (2,1), B3) Silica disk (2,1), B4) Silica rod (0.5,3), B5) Silica rod (0.25, 3), and B6) Silica rod (0.125, 3)

TABLE 3

Effective Atomic Numbers of Five Core-Sized Ge-Doped SIO_2 Optical Fibres [66]

Ge-doped SiO_2 Optical Fiber No.	Core/Cladding of Optical Fibre (μm)	Effective Atomic Number (Z_{eff})
1	100/604	13.25
2	80/483	13.69
3	60/362	13.57
4	40/241	13.40
5	20/120	13.43

that the Ge-doped SiO_2 optical fibers provided a similar Z_{eff} value, making the doped silica useful as human-bone equivalent for dosimetric purposes.

4. Reported Medical Applications

4.1 External Beam Radiotherapy

4.1.1 Thermoluminescence Response: TL dosimetry is routinely applied to verify patient doses during different types of radiotherapy worldwide [1]. It helps to increase the precision of the dose delivery to patients, affected by many variables in the overall process. The International Atomic Energy Agency (IAEA) together with the World Health Organization (WHO) have established a TLD postal program to improve the accuracy and consistency of clinical dosimetry in radiotherapy

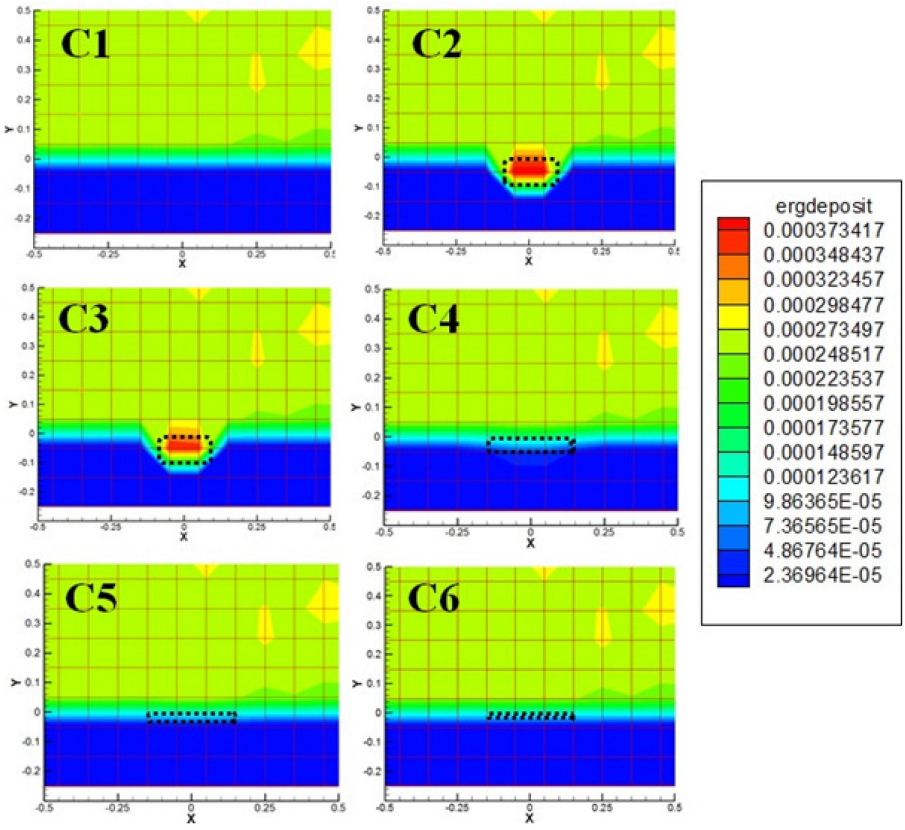

Fig. 8. Perturbation effect of various dosimeters positioned on water phantom exit surface exposed by a ^{60}Co photon beam C1) water exit surface with no dosimeter, C2) LiF disk (2,1), C3) Silica disk (2,1), C4) Silica rod (0.5,3), C5) Silica rod (0.25, 3), and C6) Silica rod (0.125,3).

centers [68]. The program supports external audits of the calibration of high-energy photon beams used in radiotherapy to trace and resolve the source of any inconsistency of the evaluated TLDs. Thus significant errors in radiotherapy dosimetry and radiological accident can be avoided. In recent years, silica fibers have attracted much attention owing to their TL characteristics with additional advantages over that of conventional TLDs including good spatial resolution ($\sim$125 μm diameter) and water resistance; both are convenient properties with regard to medical radiation dosimetry [69]–[71]. Also revealed is their significant potential as TL dosimeter materials in radiotherapy [71], including in application to brachytherapy, intensity modulated radiation therapy, micro-beam radiotherapy [72] etc.

The effects of different factors of silica fibers as a TLD were also investigated to improve TL yields in radiotherapy dosimetry. It includes the influences of several dopants [73], [74]; dopant concentration [75], [76]; core diameters [55], [66]; flat fibers [30], [77]; photonic crystal fibers/ micro structured fiber [51], [78] etc. that can deliver significant potential for megavoltage high energy beams in radiotherapy.

Ge-doped optical fiber dosimeters have been considered by [79] to verify Intensity Modulated Radiation Therapy (IMRT) three-dimensional (3D) dose distributions as shown in Fig. 9 (a) and Fig. 9 (b) respectively. For the study, two prostate cancer patients were generated using Alderson Rando Anthropomorphic Phantom CT data-sets. Measurements were performed using the Rando-phantom at nominal photon beam energies of 6 MV and 15 MV. The TL responses of Ge-doped optical fibers were compared to the treatment planning system and also with the commercial dosimeters (Harshaw TLD-100 and TLD-700). It was found that Ge- doped optical fibers exhibited

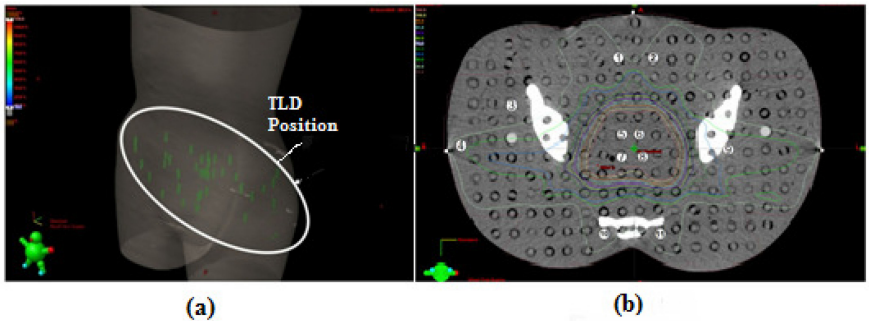

Fig. 9. (a) Ge-doped optical fibers and LiF TLDs (highlighted) in 3D view of the Rando phantom prostate CT image. (b) Numbers correspond to the positions of Ge-doped optical fibers and LiF TLDs in a Rando-phantom CT-slice [19].

good potential to verify in vitro doses within 3% of the Eclipse predicted doses and LiF TLDs for the particular high energy photon beams used.

The International Atomic Energy Agency (IAEA), World Health Organization (WHO) [80], the European Society for Therapeutic Radiology and Oncology-European Quality Assurance Network (ESTRO-EQUAL) [81], and the Radiological Physics Center (RPC) for mailed TLD systems in North America [82] applied TLDs in their IAEA/WHO TLD postal dose audit program. It has defined the acceptance limits for radiotherapy hospitals. The prescribed value is $\pm$5% following the classical tolerance value provided by the International Commission on Radiation Units and Measurements ICRU [83]. TLD based programs are gradually improving the dosimetry practices in many hospitals in developing countries in seeking to comply with the demands of modern radiotherapy dosimetry for the safe and effective delivery of radiation doses to patients. While phosphor based TLDs have hygroscopic problems [84], relatively poor spatial resolution (usually in the scale of mm) and are expensive [85], optical fiber TL material have overcome these limitations [71].

Several researchers focused on the investigation of Ge-doped optical fibers as dosimeters for postal radiotherapy dose audits of megavoltage photon beams [86], [87]. According to [86] 60 capsules each having 15 selected Ge-optical fibers were exposed to an absorbed dose to water of 2 Gy using a purpose built holder based on the IAEA TLD holder design [28] and a Qados (Sandhurst, UK) water tank. Calibration coefficient, a variety of correction factors and an uncertainty-analysis for Ge-doped silica fibers were measured consistent with the methodology recommended by [88] in the IAEA/ WHO TLD audit system. Reproducibility of Ge-doped fibers to a dose of 2Gy is represented in Fig. 10 which can be even more greatly improved using an appropriate pre-dose and heating treatment [10].

The Ge-doped optical fiber holder was identical with IAEA TLD holder whose attenuation correction factors were assessed experimentally and analytically by [89], [90]. [91] calculated the holder correction factors applying Monte Carlo simulation. Results of the simulation represented good agreement with the experimental results achieved by [89], [90]. The simulated results were applied in the study to achieve a holder correction factor for beam qualities.The Ge-doped optical fibers represented linearity between TL yield and dose, with a reproducibility of better than 5%, following repeated measurements ($n = 5$) for doses from 5 cGy to 1000 cGy. The fibers also exhibited dose rate, angular and temperature independence. Energy-dependent response was 7% above the energy range 6 MV to 15 MV (TPR20, 10 of 0.660, 0.723 and 0.774 for 6, 10 and 15 MV respectively). The audit methodology was developed with uncertainty of 4.22% at 95% confidence interval for the photon beams studied. 9 mm diameter core Ge-doped fiber revealed a viable system for application in mailed audit radiotherapy programs.

4.1.2 Radioluminescence Emission: The Radioluminescence from silica optical fibers for dosimetric purposes was suggested as early as 1981 by [92]. A pure silica fiber produced radiation-induced luminescence with emission peaks at 450 nm and 650 nm when exposed to 40 kV X-rays.

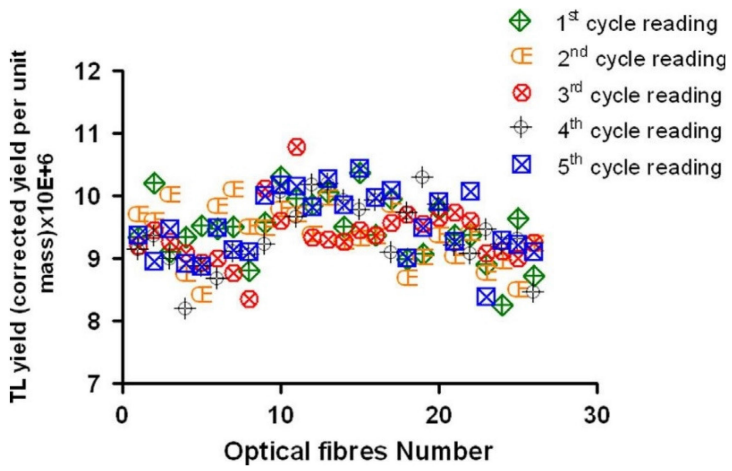

Fig. 10. Reproducibility of Ge-doped fibers following 6 MV photon beam irradiation to a dose of 2 Gy [26].

Emission at 650 nm maintained a stable level, while gradually decreasing by 25% over a radiation dose of 340 kGy. Within the same duration, the 450 nm emission increased by over an order of magnitude while showing slight tendency to stabilize on further exposure. At the time, the lack of suitable electronics and optical fiber fabrication methods did not allow rapid progress in this area.

Suggestion for Eu^{3+} doped silica optical fibers was put forth by [93] following an extensive study on potential candidates of activator ions (Dy^{3+}, Pr^{3+}, Sm^{3+}, and Tb^{3+}) and host materials for scintillating optical fibers. Eu^{3+} showed the advantage of having large emission peaks at longer wavelengths, namely, 700 nm. Based on available literature, characterization of doped silica optical fiber scintillators for remote optical dosimetry was first accomplished and formally reported by [94]. The scintillating material in this study was a Ce^{3+} doped silica core optical fiber (0.06 mol% of Ce, $\sim$175 μm core, $\sim$220 μm diameter) fabricated by the *sol-gel method*, subjected to a 20 and 32 kV ray source. Bulk SiO_2: Ce^{3+} glass had already been developed by that point following an established reputation of Ce^{3+} ions as highly-efficient luminescent centers [95]. Further investigations with this scintillator type were carried out and reported in [96]–[99]. Fig. 12 shows the radioluminescence (RL) response of Ce^{3+} doped silica core optical fiber at different dose rates.

Stem Effect has been identified as a major characteristic of fiber optic-coupled dosimetry (FOCD) systems that limits the overall accuracy of the reading. [100] experimentally showed the stem effect to consist of two *independent* components: Cerenkov radiation, and native fluorescent emission of carrier fiber. The Cerenkov radiation (angular dependent) is produced when high energy charged particles, such as electrons, cross a dielectric medium at speeds greater than the phase velocity of light in the same medium (although this is also observed for γ and X-ray source). Light pipes and optical fibers have been observed to produce both Cerenkov and fluorescence in ionizing radiation fields. In the case of FOCD, it is ideal that the only emission produced by ionizing radiation is from the scintillator that corresponds to a point in the radiation field. Stem effect phenomenon adds additional signal that varies with the length of exposed optical fiber or light pipe in the field [101]. Although most research work consider the stem effect to be noise, recently the Cerenkov component itself has been investigated for use in dose measurements [102].

Yb-doped silica optical fibers fabricated by the sol-gel method similar to Ce^{3+} doped fibers have been recently reported by [103]. As mentioned by [104], the stem effect spectrum can extend until the red region rendering the $\sim$620 nm centered RL emission of Eu^{3+} doped silica optical fiber ineffective for optical filtration method.

Pursuit of greater accuracy in dosimetric readings means development of novel methods to minimize noise in the system. Hence, characterization, and elimination or minimization of the stem

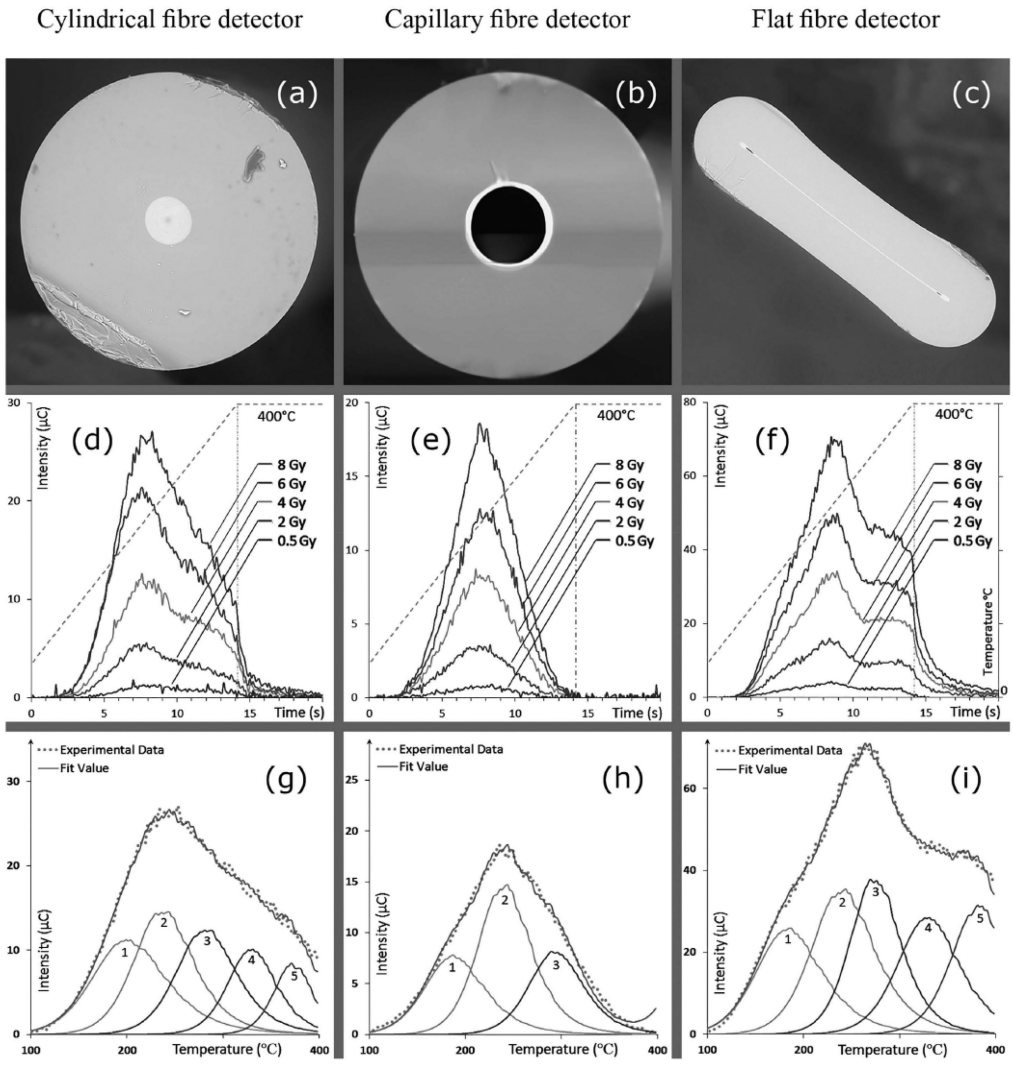

Fig. 11. Glow curve analysis. The sub-panels (a–c) are SEM cross-sectional images for the cylindrical, capillary and flat fiber, respectively; sub-panels (d–f) are the respective glow curves obtained using five different doses, provided in the form of TL intensity versus acquisition time, with temperature represented on the right-hand y-axis, and finally; sub-panels, (g–i) show the results of glow curve deconvolution calculated according to second-order kinetics modelling for the cylindrical, capillary and flat fiber respectively [45].

effect comprises a separate research area within the FOCD research domain and is as equally important as the development of novel materials with high scintillation efficiency. The most common techniques for stem effect removal are *spectral signal subtraction method* (by using signal from a reference fiber, or by using software methods to eliminate spectral data), *hollow air core method* [105], [106], *gated data acquisition method* [107]–[109], and *optical filtration method* [110]. In linear accelerator setting, the temporal discrimination of signal, or gated data acquisition technique have proven effective given the pulsed delivery nature of the radiation source. *Time-resolved dosimetry*, as the method is commonly known, makes use of electrical synchronization of linac pulses and photo-sensor operation. A trigger signal generated by the linac at the beginning of a radiation pulse delivery is sent to the photosensor. This triggers the photosensor to be inactive for a few *micro-seconds*, in essence, discarding any information for the duration when Cerenkov signal is generated. This method thus requires a scintillating material that has scintillation decay times for

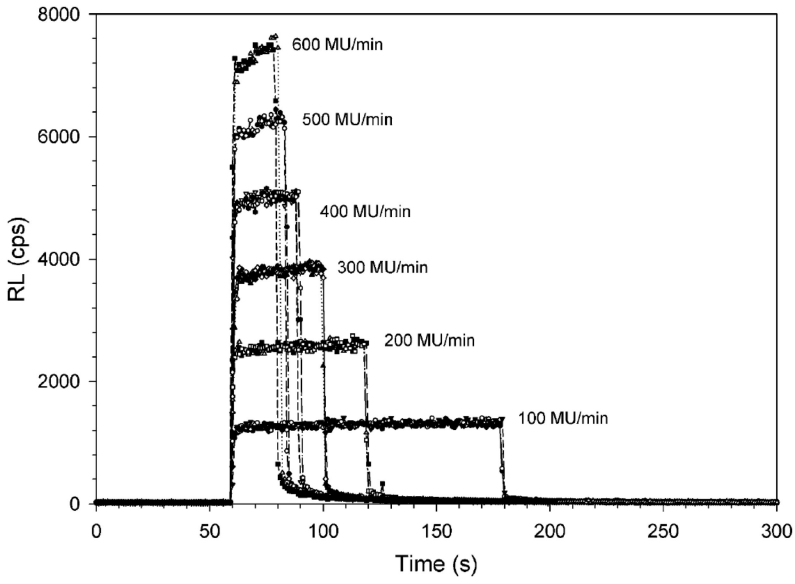

Fig. 12. RL versus time signals obtained by irradiating the fibre with a 6 MV photon beam to the same dose, using different dose rates [91].

relatively longer duration. A fully functional time-resolved FOCD was reported by [107] making use of fused quartz doped with Cu^{1+} and drawn into fibers ($\sim$400 μm overall diameter).

4.2 Brachytherapy

The delivery procedure of brachytherapy necessitates dosimeter probes with high spatial resolution. Optical fibers with their sub-mm dimensions, are therefore very suitable for this particular application (a catheter usually having an inner diameter of $\sim$1.4 mm). The challenge has been to develop materials which are linearly responsive over the respective dose and dose-rate range, being produced by common sources such as, ^{90}Sr/^{90}Y, ^{106}/Ru/^{106}Rh (beta-ray sources) and ^{125}I (low energy photon source) [111], and has sufficiently useful response per material volume. One of the earliest recorded scintillation based fiber optic coupled dosimeter probes, called *Brachy*FOD, were developed by [112] in the early 2000s. The system makes use of a commercially available BC400 blue-emitting plastic scintillator coupled to polymer fiber. Polymer fibers of 1 mm and 0.5 mm were investigated, with the larger diameter enabling better signal-to-noise ratio and lower angular dependence (^{192}Ir high dose rate source) and thus suggested for practical use (the dimensions still being less than catheter internal diameter). [113] identifies the need for stem effect (in some cases, 30% of the total signal) removal from such a system, and employs a BC60 green scintillating fiber instead of BC400 scintillator. The emission is then chromatically segregated to extract light output presumably produced only by radioluminescence, achieving improved readouts for settings when the source is relatively closer to the transmission fiber (farther from the scintillating fiber along the length of the fiber). When the source is closer to the scintillating fiber, the noise is acceptably low, thus not requiring any corrective methods.

TL response of Ge-doped silica optical fibers subjected to ^{125}I low dose rate source was investigated in [114]. The ^{125}I source used in this experiment was an OncoSeed model 6711, generally used for actual brachytherapy treatments. The distance of the radiation source and dosimeter was varied from 0.1 cm up to several cm. The results of the measurement were also compared against EGSnrc/DOSRZznrc Monte Carlo simulations and treatment planning system data. The silica fiber dosimeter showed agreement with simulations that was about 2.3% $\pm$ 0.3% along the transverse and perpendicular axes and within 3.0% $\pm$ 0.5% for measurements of anisotropy in angular dose

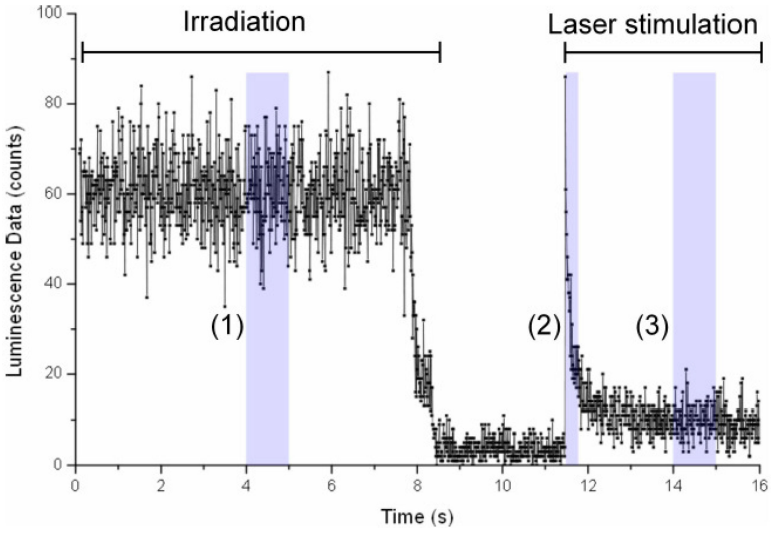

Fig. 13. Luminescence with respect to time during the measurement of OSL. Shaded regions indicate where integration of photon counts was performed in order to quantify (1) scintillation, (2) OSL, and (3) the background. Channels are of 10 ms duration [37].

distribution. Measured values and Veriseed brachytherapy treatment planning system (TPS) values were in agreement within 2.7% $\pm$ 0.5%.The Ge-doped optical fiber dosimeters also provided detailed dose mapping around brachytherapy sources of high dose gradient. [115] identified the potential use of Ge doped silica optical fibers cervix brachytherapy dose distribution measurements. In the study, the authors assessed the responses of the three different types of dosimetry system in Co-60 High Dose Rate brachytherapy including Ge doped optical fiber, EBT3 Gafchromic film and PRESAGE radiochromic plastic material. The results of the measurement were also compared with treatment planning system (TPS) calculations and Monte Carlo derived TG-43 model data. Ge doped optical fibers revealed excellent spatial resolution intended for single direction measurement however the precision regarding complete dose distribution assessment was more limited.

OSL response capabilities of optical fibers has been investigated for beta sources, although not in forms used in actual brachytherapy. Fluoride phosphate optical fiber can act as both the sensing and light guiding component of an RL/OSL system, as developed in [41]. The unclad bare optical fibers of 160 μm diameter were fabricated from commercial (Schott N-FK51A) fluoride phosphate glass. Its transmission quality was tested at the wavelength of interest 405 nm for the luminescence measurements. Transmission loss was determined to be 10 dB/m along the length of the waveguide fiber. Twenty-nine individual fibers (each 1.2 m long) were bundled in a coil of radius 45 mm. A ^{90}Sr/^{90}Y beta source was used for irradiation at a dose rate of 2 Gy/min and a green laser source of 532 nm, activated 3 s after irradiation, was selected for optical stimulation. Linear responses were obtained for accumulated dose between 0.016 and 2 Gy, with emergence of a plateau effect afterwards, and a decreasing trend beyond 8 Gy. The characteristic RL/OSL response curve is shown in Fig. 13, where the first section (1) represents the RL emission, and (2) represents the luminescence produced during the relaxation of traps by optical stimulation. [116] has extended the work on fluoride phosphate glasses, and utilizing doped silica samples prepared using the Reactive Powder Sintering of Silica (REPUSIL) process. A variety of rare-earth dopants have been investigated, namely, lanthanum (La), cerium (Ce), samarium (Sm), thulium (Tm) and Ytterbium (Yb). Of notable observations, the Ce-doped sample exhibited OSL response three orders of magnitude larger than those observed with fluoride phosphate glasses in [41]. However, the setups for these two investigations were characteristically different, with the REPUSIL process of fabrication being the most noted difference. The promise of a good dosimeter material can be found with the developed Ce-doped silica sample; however, its performance within an optical fiber geometry has yet to be investigated.

The OSL response of commercial silica optical fiber (Nokia) as a passive dosimeter was investigated under green/blue excitation laser light (480 nm) at an elevated temperature of 125 °C rather than at room temperature [117]. The fiber was cut into 5 mm long pieces. The CW-OSL response was investigated using a $^{90}Sr/^{90}Y$ beta radiation source. The commercial SiO_2 fiber exhibits linear response from 7.35 Gy to 147 Gy and the error was found to be within ∼3%. The same fiber was also studied to find OSL response when subjected to gamma radiation (^{137}Cs source, E = 0.662 MeV) from a dose range of 15.6 mGy to 93.8 mGy under 110 °C (preheat temperature). The samples were placed on a PMMA phantom located 55 cm from the gamma source. The fading imposes a time limit of around 6 days after exposure to gamma radiation, suggesting that this fiber could be used for radiological accidents or emergencies [118].

4.3 Diagnostic Radiology: Diagnostic radiology exposures are pulses of kV X-rays, often delivered in the range of a few milliseconds. The prime idea for this process is to get the sharpest images with good contrast, achieved by a combination of exposure time and radiation energy range. The optical fiber, with its sub-mm dimensions and fast electron-hole kinetics have promising potential to capture doses in such exposures accurately, without affecting the quality of images. [119] have reported a novel collapsed-hole Ge-doped PCF structure, able to capture doses as low as 0.6 mGy with TL readouts. [120] demonstrated the capabilities of Ge-B doped collapsed flat-fibers for capturing doses in the μGy range delivered by medical dental X-ray equipment (a Satelec X-Mind DC unit in this case), about two order of magnitude less than that reported for TLD-100 [121]. For the TL response for the silica media, fading has been recorded to be as much as 15% in this case, compared to 7% for that of TLD-100 commercial chips over a period of 15 days. This can be attributed to the multiple trap centers in a doped silica structure, a novel structure whose properties are vastly unexplored, compared to the established LiF. Scintillation based systems have been developed by [122] and [123] making use of a fiber optic coupled configuration with commercial scintillators. These systems are able to capture time-resolved response and produce a profile of the intensity of the pulse with respect to time. The energy range for diagnostic applications is below the threshold required for Cerenkov generation in the optical fiber setup, hence does not suffer from stem effects. The profiles of X-ray pulses in different current and voltage settings as projected by the RL response of a P-doped silica optical fiber can be found in [124]. Noted in this study is the monotonic linearity of the accumulated RL response against current-time product as well as X-ray tube peak voltage. Similar observations can be traced back to studies with Ce^{3+} doped silica optical fibers in [125]. [126] has demonstrated the usefulness of Ce-doped silica optical fiber in the diagnostic range utilizing RL and OSL methods. The sensitive material, comprising of a 3 cm Ce-doped silica rod was prepared using the sol-gel method from tetraethylorthosilicate (TEOS) precursor, showed a linear response to dose rate between 26 and 1187 mGy/s, although exhibiting a noticeable plateau effect for the first ∼75 s of exposure and a long afterglow effect. The OSL readout suffered about 50% fading in the first 6 minutes or so, being termed as “short-time fading” by the authors, before maintaining a stable level of trapped charges for the following 20 minutes. Despite the scope for under-reading or over-reading because of slow kinetic processes, the Ce-doped material appears a good candidate for real-time and online passive dosimetry in diagnostic radiology levels.

A linearity curve of response (RL and TL) vs. dose for silica optical fibers subjected to a GE Senograph DC equipment is shown in Fig. 14. Both the RL and TL responses recorded doses down to the μGy range. An advantage of the RL-based system is the ability to read data in real-time, and at multiple points simultaneously as suggested in [122], making QA programs faster and more dynamic.

5. Reported Non-medical Applications

5.1 Industrial Radiation Processing

The radiation processing industry uses radiation in the range of kGy, delivered within a span of few minutes. As reported in [127], this is a tool suited for food processing (sprouting of potatoes,

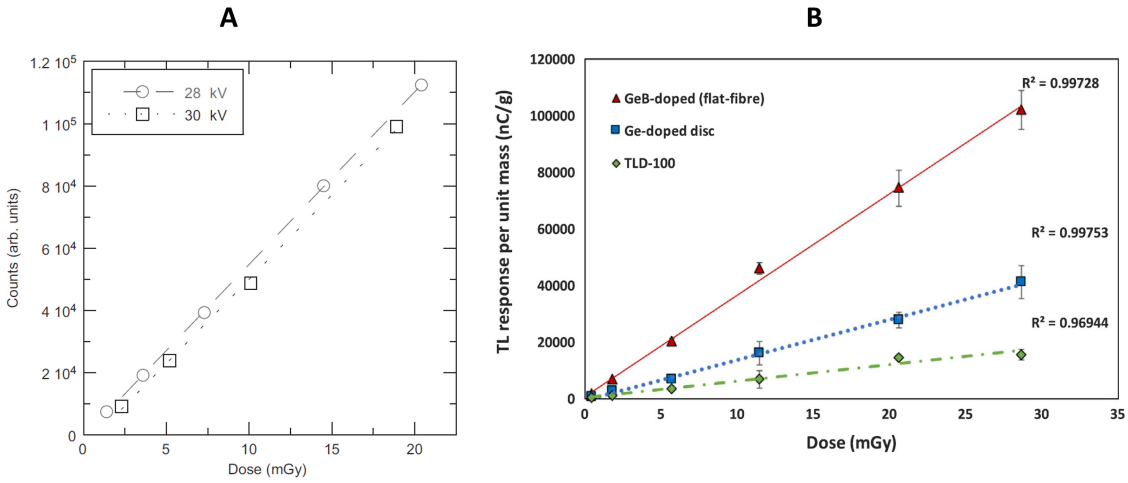

Fig. 14. (A) Ce3+ doped silica fiber RL response as a function of dose for a Senograph DS mammography system (selected voltages: 28 and 30 kV) [114], (B) TL response of Ge-B doped (flat fiber), Ge-doped rod fiber, and TLD-100 subjected to doses in the range of 0.4–28 mGy provided by a similar GE Senograph DS equipment [109].

onions and garlics; disinfestation of insects in cereals and fresh/dried fruits; delaying ripening of some fruits; elimination of pathogenic and spoilage bacteria from frozen meat etc.) was obtained by delivering gamma radiation using a 1.25 MeV Co-60 source delivering at a dose rate of 2.07 kGy/hour on samples of Ge-doped flat optical fibers (45 $\times$ 180, 60 $\times$ 270, 73 $\times$ 360, 100 $\times$ 510 and 160 $\times$ 750 μm^2 cross-section) and Ge-doped 9 μm core commercial cylindrical fibers. For delivered absorbed dose of 1 through 10 kGy, all the fibers have exhibited fair linearity of TL response ($R^2 = 0.82$), with larger dimension flat fibers having the greatest response, and smaller fibers having the least fading. A set of Ge-doped flat fibers produced in the same batch as the previous study, along with a set of undoped and Ge-B-doped fibers, were subjected to an industrial electron beam irradiation in [128] with doses upto 100 kGy. TL response of both Ge and Ge-B-doped flat fibers showed good degree of linearity with $R^2 \approx 0.97$. Of the two doped fibers, the Ge-B-doped samples yielded the greater TL signal indicating greater number of TL traps.

Effects of high doses of radiation on optical fibers have long been investigated to determine transmission capabilities of the fibers in reactor and particle accelerator environments [129], [130]. The property, called *radiation hardness*, opposes chemical changes such as photo-darkening, ensuring consistent performance of the optical fiber for data transmission. In practice, most optical fibers will suffer some deterioration in its transmission characteristics with varying effects in different bands. The induced changes in such environments can be exploited for applications such as real-time dosimetry. Doses of up to 100 kGy generated by a X-ray machine (dose rate 10.7 Gy/s on SiO_2) were delivered on P (~9 wt%) and P/Ce (9.3/2 wt%) doped SiO_2 single mode optical fibers in [131]. The RIA is monotonic with the dose and does not saturate for doses of the order of 100 kGy. The Ce co-doping with P allows a reduced sensitivity in the 1100–1900 nm region, allowing higher limits of doses in harsher environments.

5.2 Space Dosimetry

The implementation of an RIA based fiber optic dosimeter system can be found in the Navigational Technology Satellite 2 (NTS-2), launched in 1977 [132]. The setup consisted of a GaAs LED emitting at ~900nm and detected by a silicon PIN photodiode. The light intensity as such has negligible effects on the coloration of the fiber owing to radiation, allowing a non-destructive and real-time readout of the optical damage/attenuation. Measured one year after launch, the device read 6000, 600 and 350 rads for 0.52, 1.72 and 2.75 g/cm^2 Al shielding respectively. The real-time

capability enabled identifying about 2.8 times increase in dose rate from 9 rad/day to about 25 rad/day during the first half of the year, aligning with a recorded routine increase in solar activity. [133] investigated the feasibility of a Ge-P doped silica multimode fiber coil configuration (15 to 550 windings) for doses up to 100 kRad in the laboratory environment using a 1.25 MeV Co-60 source. A fiber optic based system allows expanding the limits of sensitivity by increasing the number of windings and/or adjusting the nature of light source. In space applications, thicker shielding acts as a source of secondary bremsstrahlung radiation.

[134] have made use of bare scintillating fibers to beta, X-rays, gamma rays (1 MeV), protons (50 to 300 MeV) and heavy ions (66 to 167 MeV) radiation for spacecraft components dosimetry. In contrast to the previously mentioned systems, the scintillation-based system would allow for small area/point dosimetry, with an estimated upper dose limit of 1 Mrad.

5.3 Environmental Dosimetry

A Ge-doped collapsed photonic crystal fiber, co-doped with B has been investigated by [8] for environmental dosimetry. Fiber samples of 125$\pm$10 μm diameter and 0.5$\pm$0.1 cm lengths were packed in a light-tight box, along with reference TLD-100 dosimeters and buried 20-30 cm into the soil near a rare-earth element (REE) refining facility (8 locations with radius ranging 1 to 20 km). The samples were retrieved 2, 4, 6 and 8 months post burial. The PCFc Ge (without B doping) showed the greatest response per mass, followed by PCFc Ge-B, commercial TLD-100 and TLD-200. The activity recorded was in the range of 100 to 480 μGy/y, verified with a HPGe detector. The degradation of the performance of commercial TLDs have been attributed to the presence of moisture. Such contrasts are suggestive of the robustness of silica-based dosimeter media in harsh weather conditions.

6. Limitations

Despite their very promising thermoluminescence characteristics for applications in radiation therapy dosimetry, research has shown that the Ge-doped SiO_2 optical fibers are not devoid of limitations. For instance, in a recent study of SiO_2 optical fibers as potential TLDs for radiotherapy dosimetry, [135] examined the thermoluminescence dose response of flat optical fibers of differing dimensions (i.e., 270 $\times$ 60 μm; 360 $\times$ 73 μm; 100 $\times$ 510 μm; and 160 $\times$ 750 μm), characterizing them in terms of their respective linearity, reproducibility, sensitivity to dose, as well as thermoluminescence signal loss (i.e., fading). It was found that the optical fibers thermoluminescence signal fading was approximately 20.4% 30 days post irradiation, with the loss being most rapid in the first seven days after irradiation (at approximately 17.8%) however it is known that fibres with various dopants and structures tend to show different fading due to having different depth traps. Therefore, despite their characteristic rate of loss of thermoluminescence response to fading, comparable to the conventional dosimetric materials, previous investigators such as [135] suggest that the Ge-doped SiO_2 optical fibers are still characterized by limited capability, in terms of ensuring accurate determination and measurement of radiation dose, with a linear dose "response over wide range therapeutic dose". This limitation in the Ge-doped SiO_2 optical fibers can be addressed by ensuring improved selection of the optical fibers for radiation therapy dosimetry applications.

In view of the foregoing, the Ge-doped SiO_2 optical fibers exhibit a number of thermoluminescence characteristics (i.e., high spatial resolution, water resistance, good sensitivity, reproducibility, dose rate independence, low energy dependence in MeV range, linearity of dose response in a wide range of dose, as well as a reasonable fading), such that these facets render them highly promising for radiation therapy dosimetric applications but not comprehensively so. As has been established by various investigators, including [135], the Ge-doped SiO_2 optical fibers still lack the requisite capability to ensure that radiation dose is accurately determined and measured with a linear dose response over a wide range therapeutic dose, soft tissue equivalence being one marked issue. In this latter regard, there is need for further research to devise ways of addressing such limitation. In particular, there is need for active and passive dosimeters of small dimensions,

with facets similar to that of the silica media but that which in addition offer soft-tissue equivalence, pointing the way to dosimetry of low keV photon fields.

7. Conclusion

In this review, the many highly favourable dosimetric characteristics of promising silica optical fibers, doped and undoped, have been covered. Aspects of fabrication, materials, dimensions and geometry of the optical fiber radiation dosimeter have also been discussed. The various applications reviewed include external beam radiotherapy, brachytherapy, diagnostic imaging, industrial radiation processing, cosmic radiation and NORM (environmental) measurements. Various techniques, individually or as combined, have been deployed to measure radiation doses from μGy to kGy, at varying dose-rates. We discussed the limitations of such dosimeters and envisage future developments in optical fiber radiation dosimetry, including use within both the pristine environment as well as in the minerals and oil and gas extractive industries where technologically enhanced natural occurring radioactive material can present a problem.

Acknowledgment

The authors wish to thank the anonymous reviewers for their valuable suggestions.

References

[1] Y. A. Abdulla, Y. M. Amin, and D. A. Bradley, "The thermoluminescence response of Ge-doped optical fibre subjected to photon irradiation," vol. 61, pp. 409–410, 2001.
[2] A. L. Yusoff, R. P. Hugtenburg, and D. A. Bradley, "Review of development of a silica-based thermoluminescence dosimeter," *Radiat. Phys. Chem.*, vol. 74, no. 6, pp. 459–481, Dec. 2005.
[3] G. Espinosa, J. I. Golzarri, J. Bogard, and J. García-Macedo, "Commercial optical fibre as TLD material," *Radiat. Prot. Dosimetry*, vol. 119, no. 1–4, pp. 197–200, 2006.
[4] A. Huston, B. Justus, P. Falkenstein, R. Miller, H. Ning, and R. Altemus, "Remote optical fiber dosimetry," *Nucl. Instruments Methods Phys. Res. Sect. B Beam Interact. with Mater. Atoms*, vol. 184, no. 1–2, pp. 55–67, 2001.
[5] L. A. Benevides, A. L. Huston, B. L. Justus, P. Falkenstein, L. F. Brateman, and D. E. Hintenlang, "Characterization of a fiber-optic-coupled radioluminescent detector for application in the mammography energy range," *Med. Phys.*, vol. 34, no. 6, pp. 2220–2227, 2007.
[6] B. L. Justus, S. Rychnovsky, M. A. Miller, K. J. Pawlovich, and A. L. Huston, "Optically stimulated luminescence radiation dosimetry using doped silica glass," *Radiat. Prot. Dosimetry*, vol. 74, no. 3, pp. 151–154, 1997.
[7] M. C. Aznar *et al.*, "Real-time optical-fibre luminescence dosimetry for radiotherapy: Physical characteristics and applications in photon beams," *Phys. Med. Biol.*, vol. 49, no. 9, pp. 1655–1669, 2004.
[8] Z. S. Rozaila *et al.*, "Environmental monitoring through use of silica-based TLD," *J. Radiol. Prot.*, vol. 37, no. 3, pp. 761–779, 2017.
[9] N. M. Noor, N. A. Shukor, M. Hussein, A. Nisbet, and D. A. Bradley, "Comparison of the TL fading characteristics of Ge-doped optical fibres and LiF dosimeters," *Appl. Radiat. Isot.*, vol. 70, no. 7, pp. 1384–1387, 2012.
[10] F. Moradi *et al.*, "Influence of dose history on thermoluminescence response of Ge-doped silica optical fibre dosimeters," *Radiat. Phys. Chem.*, vol. 134, no. Aug. 2016, pp. 62–70, 2017.
[11] F. Moradi *et al.*, "Evaluation of Ge-doped silica fibre TLDs for in vivo dosimetry during intraoperative radiotherapy," *Phys. Med. Biol.*, vol. 64, no. 8, 2019.
[12] C. Soares *et al.*, "Absorbed dose measurements of a handheld 50 kVP X-ray source in water with thermoluminescence dosemeters," *Radiat. Prot. Dosimetry*, vol. 120, no. 1–4, pp. 78–82, 2006.
[13] H. Bouchard, Y. Kamio, H. Palmans, J. Seuntjens, and S. Duane, "Detector dose response in megavoltage small photon beams. II. Pencil beam perturbation effects," *Med. Phys.*, vol. 42, no. 10, pp. 6048–6061, 2015.
[14] S. W. S. Mckeever and R. Chen, "Luminescence models," *Radiat. Meas.*, vol. 27, no. 5–6, pp. 625–661, 1997.
[15] D. L. Griscom and E. J. Friebele, "Effects of ionizing radiation on amorphous insulators," *Radiat. Eff.*, vol. 65, pp. 63–72, 1982.
[16] D. Ehrt and W. Vogel, "Radiation effects in glasses," *Nucl. Inst. Methods Phys. Res. B*, vol. 65, no. 1–4, pp. 1–8, 1992.
[17] M. N. Ott, "Fiber optic cable assemblies for space flight: II. Thermal and radiation effects," in *Proc. SPIE*, 1998, vol. 3440.
[18] M. Alam, J. Abramczyk, J. Farroni, U. Manyam, and D. Guertin, "Passive and active optical fibers for space and terrestrial applications," *Photonics Sp. Environ. XI*, vol. 6308, no. 860, p. 630808, 2006.
[19] O. Deparis, D. L. Griscom, P. Mégret, M. Decréton, and M. Blondel, "Influence of the cladding thickness on the evolution of the NBOHC band in optical fibers exposed to gamma radiations," *J. Non. Cryst. Solids*, vol. 216, pp. 124–128, 1997.
[20] M. Alam *et al.*, "Fiber amplifier performance in γ-radiation environment," in *Proc. Opt. Fiber Commun. Conf. Exp. Nat. Fiber Opt. Engineers Conf.*, 2007, vol. 3, no. 1, pp. 7–9.

[21] P. F. Kashaykin, A. L. Tomashuk, M. Y. Salgansky, A. N. Guryanov, and E. M. Dianov, "Influence of drawing conditions on radiation-induced attenuation of pure-silica-core fibers in the near-IR range," in *Proc. SPIE*, 2018, vol. 10681.
[22] A. J. J. Bos, "On the energy conversion in thermoluminescence dosimetry materials," *Radiat. Meas.*, vol. 33, no. 5, pp. 737–744, 2001.
[23] A. F. McKinlay, *Thermoluminescence dosimetry*. United Kingdom: Adam Hilger, 1981.
[24] D. W. Cooke and J. F. Rhodes, "Thermoluminescence studies of LiF (TLD-100) in the temperature interval 10–300 K," *J. Appl. Phys.*, vol. 52, no. 6, pp. 4244–4247, Jun. 1981.
[25] R. G. Fairchild, P. L. Mattern, K. Lengweiler, and P. W. Levy, "Thermoluminescence of LiF TLD-100: Glow-curve kinetics," *J. Appl. Phys.*, vol. 49, no. 8, pp. 4523–4533, Aug. 1978.
[26] S. W. S. McKeever, *Thermoluminescence of Solids*. Cambridge: Cambridge University Press, 1985.
[27] G. A. Dussel and R. H. Bube, "Theory of Thermally Stimulated Conductivity in a Previously Photoexcited Crystal," *Phys. Rev.*, vol. 155, no. 3, pp. 764–779, Mar. 1967.
[28] A. T. Abdul Rahman *et al.*, "An investigation of the thermoluminescence of Ge-doped SiO_2 optical fibres for application in interface radiation dosimetry," *Appl. Radiat. Isot.*, vol. 70, no. 7, pp. 1436–1441, 2012.
[29] F. Issa, N. Atiqah, A. Latip, D. A. Bradley, and A. Nisbet, "Ge-doped optical fibres as thermoluminescence dosimeters for kilovoltage X-ray therapy irradiations," *Nucl. Inst. Methods Phys. Res. A*, vol. 652, no. 1, pp. 834–837, 2011.
[30] S. Hashim *et al.*, "Thermoluminescence response of flat optical fiber subjected to 9 MeV electron irradiations," *Radiat. Phys. Chem.*, vol. 106, pp. 46–49, 2015.
[31] A. T. A. Rahman, A. Nisbet, and D. A. Bradley, "Dose-rate and the reciprocity law: TL response of Ge-doped SiO_2 optical fibers at therapeutic radiation doses," *Nucl. Inst. Methods Phys. Res. A*, vol. 652, no. 1, pp. 891–895, 2011.
[32] M. F. Hassan *et al.*, "The thermoluminescence response of Ge-doped flat fibre for proton beam measurements: A preliminary study," *J. Phys. Conf. Ser.*, vol. 851, no. 1, 2017.
[33] A. T. Ramli, D. A. Bradley, S. Hashim, and H. Wagiran, "The thermoluminescence response of doped SiO_2 optical fibres subjected to alpha-particle irradiation," *Appl. Radiat. Isot.*, vol. 67, no. 3, pp. 428–432, 2009.
[34] S. Hashim, D. A. Bradley, M. I. Saripan, A. T. Ramli, and H. Wagiran, "The thermoluminescence response of doped SiO_2 optical fibres subjected to fast neutrons," *Appl. Radiat. Isot.*, vol. 68, no. 4–5, pp. 700–703, 2010.
[35] A. Entezam, M. U. Khandaker, Y. M. Amin, N. M. Ung, J. Maah, and D. A. Bradley, "Thermoluminescence response of Ge-doped SiO_2 fibres to electrons, X- and γ-radiation," *Radiat. Phys. Chem.*, vol. 121, pp. 115–121, 2016.
[36] M. Begum *et al.*, "Thermoluminescence response of Ge-doped optical fiber dosimeters with different core sizes," in *Proc. 4th Int. Conf. Photon.*, 2013, pp. 291–293.
[37] E. G. Yukihara and S. W. S. McKeever, *Optically Stimulated Luminescence*. Hoboken, NJ, USA: Wiley, 2011.
[38] K. A. Mat-Sharif *et al.*, "Effect of GeCl4/SiCl4 flow ratio on germanium incorporation in MCVD process," in *Proc. 4th Int. Conf. Photon.*, 2013, pp. 284–287.
[39] S. Nagel, J. MacChesney, and K. Walker, "An overview of the modified chemical vapor deposition (MCVD) process and performance," *IEEE J. Quantum Electron.*, vol. 18, no. 4, pp. 459–476, Apr. 1982.
[40] H. Ebendorff-Heidepriem and T. M. Monro, "Extrusion of complex preforms for microstructured optical fibers," *Opt. Express*, vol. 15, no. 23, p. 15086, 2007.
[41] C. A. G. Kalnins, H. Ebendorff-Heidepriem, N. A. Spooner, and T. M. Monro, "Radiation dosimetry using optically stimulated luminescence in fluoride phosphate optical fibres," *Opt. Mater. Express*, vol. 2, no. 1, p. 62, 2012.
[42] T. Rivera, C. Furetta, J. Azorín, M. Barrera, and A. M. Soto, "Thermoluminescence (TL) of europium-doped ZrO2 obtained by sol-gel method," *Radiat. Eff. Defects Solids*, vol. 162, no. 5, pp. 379–383, 2007.
[43] J. E. Townsend, S. B. Poole, and D. N. Payne, "Solution-doping technique for fabrication of rare-earth-doped optical fibres," *Electron. Lett.*, vol. 23, no. 7, p. 329, 1987.
[44] A. Dhar *et al.*, "Characterization of porous core layer for controlling rare earth incorporation in optical fiber," *Opt. Express*, vol. 14, no. 20, p. 9006, 2006.
[45] A. Dhar, A. Pal, M. C. Paul, P. Ray, H. S. Maiti, and R. Sen, "The mechanism of rare earth incorporation in solution doping process," *Opt. Express*, vol. 16, no. 17, pp. 12835–12846, 2008.
[46] V. F. Khopin, A. A. Umnikov, A. N. Gur'yanov, M. M. Bubnov, A. K. Senatorov, and E. M. Dianov, "Doping of optical fiber preforms via porous silica layer infiltration with salt solutions," *Inorg. Mater.*, vol. 41, no. 3, pp. 303–307, Mar. 2005.
[47] J. Kirchhof, S. Unger, and A. Schwuchow, "Fiber lasers: materials, structures and technologies," *Opt. Fibers Sensors Med. Appl. III*, vol. 4957, pp. 1–15, 2003.
[48] V. Petit, A. Le Rouge, F. Béclin, H. El Hamzaoui, and L. Bigot, "Experimental study of SiO_2 soot deposition using the outside vapor deposition method," *Aerosol Sci. Technol.*, vol. 44, no. 5, pp. 388–394, 2010.
[49] M. Ghomeishi, G. A. Mahdiraji, F. R. M. Adikan, N. M. Ung, and D. A. Bradley, "Sensitive Fibre-Based Thermoluminescence Detectors for High Resolution In-Vivo Dosimetry," *Sci. Rep.*, vol. 5, pp. 1–10, 2015.
[50] M. Begum *et al.*, "Comparison of thermoluminescence response of different sized Ge-doped flat fibers as a dosimeter," *Radiat. Phys. Chem.*, vol. 116, pp. 155–159, 2015.
[51] E. Dermosesian, G. Amouzad Mahdiraji, F. R. Mahamd Adikan, and D. A. Bradley, "Improving thermoluminescence response through the fabrication of novel microstructured fibers," *Radiat. Phys. Chem.*, vol. 116, pp. 135–137, 2015.
[52] G. A. Mahdiraji, F. R. M. Adikan, and D. A. Bradley, "Collapsed optical fiber: A novel method for improving thermoluminescence response of optical fiber," *J. Lumin.*, vol. 161, pp. 442–447, 2015.
[53] M. Benabdesselam *et al.*, "Performance of ge-doped optical fiber as a thermoluminescent dosimeter," *IEEE Trans. Nucl. Sci.*, vol. 60, no. 6, pp. 4251–4256, 2013.
[54] S. Hashim, M. I. Saripan, A. T. A. Rahman, N. H. Yaakob, D. A. Bradley, and K. Alzimami, "Effective atomic number of Ge-doped and Al-doped optical fibers for radiation dosimetry purposes," *IEEE Trans. Nucl. Sci.*, vol. 60, no. 2, pp. 555–559, 2013.
[55] N. A. Zahaimi *et al.*, "Dopant concentration and thermoluminescence (TL) properties of tailor-made Ge-doped SiO_2 fibres," *Radiat. Phys. Chem.*, vol. 104, pp. 297–301, 2014.
[56] G. A. Mahdiraji *et al.*, "Sensors and Actuators A: Physical Optical fiber based dosimeter sensor: Beyond TLD-100 limits," *Sensors Actuators A. Phys.*, vol. 222, pp. 48–57, 2015.

[57] N. Wahib *et al.*, "Gamma irradiated thermoluminescence response of Ge-doped SiO_2 fibre," *Appl. Radiat. Isot.*, vol. 105, pp. 158–162, 2015.
[58] A. Alawiah, M. M. Fadhli, S. Bauk, H. A. Abdul-Rashid, and M. J. Maah, " Assessment of GeB doped SiO_2 optical fiber for the application of remote radiation sensing system," *Micro/Nano Mater. Devices, Syst.*, vol. 8923, 2013, Art. no. 89235F.
[59] N. H. Yaakob *et al.*, "Electron irradiation response on Ge and Al-doped SiO_2 optical fibres," *Nucl. Instruments Methods Phys. Res. Sect. A Accel. Spectrometers, Detect. Assoc. Equip.*, vol. 637, no. 1, pp. 185–189, 2011.
[60] F. Moradi *et al.*, "Investigation on various types of silica fibre as thermoluminescent sensors for ultra-high dose radiation dosimetry," *Sensors Actuators, A Phys.*, vol. 273, pp. 197–205, 2018.
[61] A. L. Tomashuk, M. V. Grekov, S. A. Vasiliev, and V. V. Svetukhin, "Fiber-optic dosimeter based on radiation-induced attenuation in P-doped fiber: Suppression of post-irradiation fading by using two working wavelengths in visible range," *Opt. Express*, vol. 22, no. 14, pp. 16778–16783, 2014.
[62] A. Alawiah *et al.*, "The thermoluminescence characteristics and the glow curves of Thulium doped silica fiber exposed to 10 MV photon and 21 MeV electron radiation," *Appl. Radiat. Isot.*, vol. 98, pp. 80–86, 2015.
[63] G. A. Mahdiraji, M. Ghomeishi, F. R. M. Adikan, and D. A. Bradley, "Influence of optical fiber diameter on thermoluminescence response," *Radiat. Phys. Chem.*, vol. 140, pp. 2–10, 2017.
[64] S. E. Lam, D. A. Bradley, R. Mahmud, M. Pawanchek, H. A. Abdul Rashid, and N. Mohd Noor, "Dosimetric characteristics of fabricated Ge-doped silica optical fibre for small-field dosimetry," *Results Phys.*, vol. 12, no. Dec. 2018, pp. 816–826, 2019.
[65] H. Asni *et al.*, "Thermoluminescence Energy Response of Germanium Doped Optical Fibre Using Monte Carlo N-Particle Code Simulation," 2010, pp. 420–423.
[66] M. Begum *et al.*, "Thermoluminescence characteristics of Ge-doped optical fibers with different dimensions for radiation dosimetry," *Appl. Radiat. Isot.*, vol. 100, pp. 79–83, 2015.
[67] Bradley*et al.*, "Doped silica fibre thermoluminescence measurements of radiation dose in the use of 223 Ra," *Appl. Radiat. Isot.*, vol. 138, pp. 65–72, Aug. 2018.
[68] J. Izewska, P. Andreo, S. Vatnitsky, and K. R. Shortt, "The IAEA/WHO TLD postal dose quality audits for radiotherapy: A perspective of dosimetry practices at hospitals in developing countries," *Radiother. Oncol.*, vol. 69, no. 1, pp. 91–97, 2003.
[69] S. F. Abdul Sani *et al.*, "XPS and PIXE analysis of doped silica fibre for radiation dosimetry," *J. Lightw. Technol.*, vol. 33, no. 11, pp. 2268–2278, 2015.
[70] D. A. Bradley *et al.*, "Review of doped silica glass optical fibre: Their TL properties and potential applications in radiation therapy dosimetry," *Appl. Radiat. Isot.*, vol. 71, pp. 2–11, 2012.
[71] C. L. Ong, S. Kandaiya, H. T. Kho, and M. T. Chong, "Segments of a commercial Ge-doped optical fiber as a thermoluminescent dosimeter in radiotherapy," *Radiat. Meas.*, vol. 44, no. 2, pp. 158–162, 2009.
[72] "Feasibility of employing thick microbeams from superficial and orthovoltage kVp x-ray tubes for radiotherapy of superficial cancers," *Radiat. Phys. Chem.*, vol. 140, pp. 237–241, 2017.
[73] M. H. Sahini, I. Hossain, H. Wagiran, M. A. Saeed, and H. Ali, "Thermoluminescence responses of the Yb- and Yb-Tb-doped SiO_2 optical fibers to 6-MV photons," *Appl. Radiat. Isot.*, vol. 92, pp. 18–21, 2014.
[74] S. Hashim, D. A. Bradley, N. Peng, A. T. Ramli, and H. Wagiran, "The thermoluminescence response of oxygen-doped optical fibres subjected to photon and electron irradiations," in *Proc. Nuclear Instruments and Methods in Physics Research, Section A: Accelerators, Spectrometers, Detectors and Associated Equipment*, 2010.
[75] M. Begum *et al.*, "The effect of different dopant concentration of tailor-made silica fibers in radiotherapy dosimetry," *Radiat. Phys. Chem.*, vol. 141, pp. 73–77, 2017.
[76] N. M. Noor *et al.*, "Radiotherapy dosimetry and the thermoluminescence characteristics of Ge-doped fibres of differing germanium dopant concentration and outer diameter," *Radiat. Phys. Chem.*, vol. 126, pp. 56–61, 2016.
[77] M. Begum, A. K. M. M. Rahman, M. Begum, H. A. Abdul-Rashid, Z. Yusoff, and D. A. Bradley, "Harnessing the thermoluminescence of Ge-doped silica flat-fibres for medical dosimetry," *Sensors Actuators, A Phys.*, vol. 270, pp. 170–176, 2018.
[78] S. Hashim *et al.*, "Photon irradiation response of photonic crystal fibres and flat fibres at radiation therapy doses," *Appl. Radiat. Isot.*, vol. 90, pp. 258–260, 2014.
[79] N. M. Noor, M. Hussein, D. A. Bradley, and A. Nisbet, "Investigation of the use of Ge-doped optical fibre for in vitro IMRT prostate dosimetry," *Nucl. Instruments Methods Phys. Res. Sect. A Accel. Spectrometers, Detect. Assoc. Equip.*, vol. 652, no. 1, pp. 819–823, 2011.
[80] J. Izewska and P. Andreo, "The IAEA/WHO TLD postal programme for radiotherapy hospitals," *Radiother. Oncol.*, vol. 54, no. 1, pp. 65–72, 2000.
[81] F. I. H., D. A., B. A., C. J., and S. H., "The ESTRO-QUALity assurance network (EQUAL)," *Radiother. Oncol.*, vol. 55, no. 3, pp. 273–284, 2000.
[82] D. A. Johnston, "Uncertainty analysis of absorbed dose calculations from thermoluminescence dosimeters," *Med. Phys.*, vol. 19, no. 6, pp. 1427–1433, 1992.
[83] ICRU, "Determination of absorbed dose in a patient irradiated by beams of X or gamma rays in radiotherapy procedures," Bethesda, MD, 1976.
[84] S. Hashim *et al.*, "The thermoluminescence response of doped SiO_2 optical fibres subjected to photon and electron irradiations," *Appl. Radiat. Isot.*, vol. 67, pp. 423–427, 2009.
[85] J. E. Rah, J. Y. Hong, G. Y. Kim, Y. L. Kim, D. O. Shin, and T. S. Suh, "A comparison of the dosimetric characteristics of a glass rod dosimeter and a thermoluminescent dosimeter for mailed dosimeter," *Radiat. Meas.*, vol. 44, no. 1, pp. 18–22, 2009.
[86] N. M. Noor, M. Hussein, T. Kadni, D. A. Bradley, and A. Nisbet, "Characterization of Ge-doped optical fibres for MV radiotherapy dosimetry," *Radiat. Phys. Chem.*, vol. 98, pp. 33–41, 2014.
[87] M. S. A. Fadzil *et al.*, "Dosimetric characteristics of fabricated silica fibre for postal radiotherapy dose audits," *J. Phys. Conf. Ser.*, vol. 546, no. 1, 2014.

[88] J. Izewska, M. Hultqvist, and P. Bera, "Analysis of uncertainties in the IAEA/WHO TLD postal dose audit system," *Radiat. Meas.*, vol. 43, no. 2–6, pp. 959–963, 2008.
[89] J. Izewska *et al.*, "A methodology for TLD postal dosimetry audit of high-energy radiotherapy photon beams in non-reference conditions," *Radiother. Oncol.*, vol. 84, no. 1, pp. 67–74, 2007.
[90] J. Izewska, J. Novotny, J. Van Dam, A. Dutreix, and E. van der Schueren, "The influence of the IAEA standard holder on dose evaluated from TLD samples," *Phys. Med. Biol.*, vol. 41, no. 3, pp. 465–473, Mar. 1996.
[91] M. Hultqvist, J. M. Fernndez-Varea, and J. Izewska, "Monte carlo simulation of correction factors for IAEA TLD holders," *Phys. Med. Biol.*, vol. 55, no. 6, 2010.
[92] M. J. Marrone, "Radiation-induced luminescence in silica core optical fibers," *Appl. Phys. Lett.*, vol. 38, no. 3, pp. 115–117, 1981.
[93] E. Takada, Y. Hosono, T. Kakuta, M. Yamazaki, H. Takahashi, and M. Nakazawa, "Application of red and near infrared emission from rare earth ions for radiation measurements based on optical fibers," vol. 45, no. 3, pp. 556–560, 1998.
[94] A. Vedda *et al.*, "Ce3+ -doped fibers for remote radiation dosimetry," *Appl. Phys. Lett.*, vol. 85, no. 26, pp. 6356–6358, 2004.
[95] N. Chiodini *et al.*, "High-efficiency SiO_2:Ce3+ glass scintillators," *Appl. Phys. Lett.*, vol. 81, no. 23, pp. 4374–4376, 2002.
[96] E. Mones *et al.*, "Feasibility study for the use of Ce3+-doped optical fibres in radiotherapy," *Nucl. Instruments Methods Phys. Res. Sect. A Accel. Spectrometers, Detect. Assoc. Equip.*, vol. 562, no. 1, pp. 449–455, 2006.
[97] N. Chiodini *et al.*, "Ce doped SiO_2 optical fibers for remote radiation sensing and," *Fiber Opt. Sensors Appl. VI*, vol. 7316, pp. 1–8, 2009.
[98] I. Veronese *et al.*, "Feasibility study for the use of cerium-doped silica fibres in proton therapy," *Radiat. Meas.*, vol. 45, no. 3–6, pp. 635–639, Mar. 2010.
[99] I. Veronese *et al.*, "Study of the radioluminesence spectra of doped silica optical fibre dosimeters for stem effect removal," *J. Phys. D. Appl. Phys.*, vol. 46, no. 1, 2013.
[100] S. F. de Boer, A. S. Beddar, and J. A. Rawlinson, "Optical filtering and spectral measurements of radiation-induced light in plastic scintillation dosimetry," *Phys. Med. Biol.*, vol. 38, no. 7, pp. 945–958, 1993.
[101] A. S. Beddar, T. R. Mackie, and F. H. Attix, "Cerenkov light generated in optical fibres and other light pipes irradiated by electron beams," *Phys. Med. Biol.*, vol. 37, no. 4, pp. 925–935, 1992.
[102] A. K. Glaser, R. Zhang, D. J. Gladstone, and B. W. Pogue, "Optical dosimetry of radiotherapy beams using Cherenkov radiation: The relationship between light emission and dose," *Phys. Med. Biol.*, vol. 59, no. 14, pp. 3789–3811, 2014.
[103] I. Veronese *et al.*, "Infrared luminescence for real time ionizing radiation detection," *Appl. Phys. Lett.*, vol. 105, no. 6, pp. 1–5, 2014.
[104] I. Veronese *et al.*, "The influence of the stem effect in Eu-doped silica optical fibres," *Radiat. Meas.*, vol. 56, pp. 316–319, Sep. 2013.
[105] P. Z. Y. Liu, N. Suchowerska, J. Lambert, P. Abolfathi, and D. R. McKenzie, "Plastic scintillation dosimetry: Comparison of three solutions for the Cerenkov challenge," *Phys. Med. Biol.*, vol. 56, no. 18, pp. 5805–5821, 2011.
[106] J. Lambert, Y. Yin, D. R. McKenzie, S. Law, and N. Suchowerska, "Cerenkov-free scintillation dosimetry in external beam radiotherapy with an air core light guide," *Phys. Med. Biol.*, vol. 53, no. 11, pp. 3071–3080, 2008.
[107] B. L. Justus, P. Falkenstein, A. L. Huston, M. C. Plazas, H. Ning, and R. W. Miller, "Gated Fiber-Optic-Coupled Detector for In Vivo Real-Time Radiation Dosimetry," *Appl. Opt.*, vol. 43, no. 8, pp. 1663–1668, 2004.
[108] T. Teichmann, J. Sponner, J. Radtke, and J. Henniger, "Gated discrimination of the stem signal in pulsed radiation fields for a fiber optic dosimetry system based on the radioluminescence of beryllium oxide," *Radiat. Meas.*, vol. 106, pp. 552–555, 2017.
[109] M. A. Clift, P. N. Johnston, and D. V. Webb, "A temporal method of avoiding the Cerenkov radiation generated in organic scintillator dosimeters by pulsed mega-voltage electron and photon beams," *Phys. Med. Biol.*, vol. 47, no. 8, pp. 1421–1433, 2002.
[110] J. M. Fontbonne *et al.*, "Scintillating fiber dosimeter for radiation therapy accelerator," *IEEE Trans. Nucl. Sci.*, vol. 49 I, no. 5, pp. 2223–2227, 2002.
[111] "Sources and Their Application in Brachytherapy," *J. ICRU*, vol. 4, no. 2, pp. 21–28, 2004.
[112] J. Lambert, D. R. McKenzie, S. Law, J. Elsey, and N. Suchowerska, "A plastic scintillation dosimeter for high dose rate brachytherapy," *Phys. Med. Biol.*, vol. 51, no. 21, pp. 5505–5516, 2006.
[113] F. Therriault-Proulx, S. Beddar, T. M. Briere, L. Archambault, and L. Beaulieu, "Technical note: Removing the stem effect when performing Ir-192 HDR brachytherapy in vivo dosimetry using plastic scintillation detectors: A relevant and necessary step," *Med. Phys.*, vol. 38, no. 4, pp. 2176–2179, 2011.
[114] F. Issa, R. P. Hugtenburg, A. Nisbet, and D. A. Bradley, "Novel high resolution 125I brachytherapy source dosimetry using Ge-doped optical fibres," *Radiat. Phys. Chem.*, vol. 92, pp. 48–53, 2013.
[115] A. L. Palmer *et al.*, "Comparison of methods for the measurement of radiation dose distributions in high dose rate (HDR) brachytherapy: Ge-doped optical fiber, EBT3 Gafchromic film, and PRESAGE radiochromic plastic," *Med. Phys.*, vol. 40, no. 6, pp. 1–11, 2013.
[116] R. E. Shaw *et al.*, "Luminescence effects in reactive powder sintered silica glasses for radiation sensing," *J. Am. Ceram. Soc.*, vol. 102, no. 1, pp. 222–238, 2019.
[117] G. Espinosa and J. S. Bogard, "Optically stimulated luminescence response of commercial SiO_2 optical fiber," *J. Radioanal. Nucl. Chem.*, vol. 277, no. 1, pp. 125–129, 2008.
[118] G. Espinosa, "A study and characterization of the optically stimulated luminescence response of commercial SiO_2 optical fiber to gamma radiation," *Rev. Mex. Física*, vol. 57, Feb. 2011, pp. 30–33, 2011.
[119] G. Amouzad Mahdiraji, E. Dermosesian, M. J. Safari, F. R. Mahamd Adikan, and D. A. Bradley, "Collapsed-Hole Ge-Doped Photonic Crystal Fiber as a Diagnostic Radiation Dosimeter," *J. Light. Technol.*, vol. 33, no. 16, pp. 3439–3445, 2015.
[120] A. Alyahyawi, T. Jupp, M. Alkhorayef, and D. A. Bradley, "Tailor-made Ge-doped silica-glass for clinical diagnostic X-ray dosimetry," *Appl. Radiat. Isot.*, vol. 138, pp. 45–49, Aug. 2018.

[121] K. Burke and D. Sutton, "Optimization and deconvolution of lithium fluoride TLD-100 in diagnostic radiology," *Brit. J. Radiol.*, vol. 70, pp. 261–271, 1997.
[122] D. E. Hyer, R. F. Fisher, and D. E. Hintenlang, "Characterization of a water-equivalent fiber-optic coupled dosimeter for use in diagnostic radiology," *Med. Phys.*, vol. 36, no. 5, pp. 1711–1716, 2009.
[123] W. J. Yoo *et al.*, "Development of a scintillating fiber-optic dosimeter for measuring the entrance surface dose in diagnostic radiology," *Radiat. Meas.*, vol. 48, no. 1, pp. 29–34, 2013.
[124] D. A. Bradley *et al.*, "Radioluminescence sensing of radiology exposures using P-doped silica optical fibres," *Appl. Radiat. Isot.*, vol. 141, pp. 176–181, 2018.
[125] N. Caretto, N. Chiodini, F. Moretti, D. Origgi, G. Tosi, and A. Vedda, "Feasibility of dose assessment in radiological diagnostic equipments using Ce-doped radio-luminescent optical fibers," *Nucl. Instruments Methods Phys. Res. Sect. A Accel. Spectrometers, Detect. Assoc. Equip.*, vol. 612, no. 2, pp. 407–411, 2010.
[126] N. Al Helou *et al.*, "Radioluminescence and optically stimulated luminescence responses of a cerium-doped sol-gel silica glass under X-Ray Beam Irradiation," *IEEE Trans. Nucl. Sci.*, vol. 65, no. 8, pp. 1591–1597, 2018.
[127] N. M. Noor, M. A. Jusoh, A. F. A. Razis, A. Alawiah, and D. A. Bradley, "Flat Ge-doped optical fibres for food irradiation dosimetry," in *Proc. AIP Conf.*, 2015, vol. 1657.
[128] H. Ahmad Tajuddin, W. M. S. Wan Hassan, S. F. Abdul Sani, and S. A. Hashim, "Development of optical fibers for food irradiation dosimeter," *Malaysian J. Fundam. Appl. Sci.*, vol. 15, no. 1, pp. 109–111, 2019.
[129] T. Kakuta *et al.*, "Radiation Resistance Characteristics of Optical Fibers," *J. Lightw. Technol.*, vol. 4, no. 8, pp. 1139–1143, 1986.
[130] T. Kakuta, T. Shikama, M. Narui, and T. Sagawa, "Behavior of optical fibers under heavy irradiation," *Fusion Eng. Des.*, vol. 41, no. 1–4, pp. 201–205, 1998.
[131] D. Di Francesca *et al.*, "Radiation-Induced Attenuation in Single-Mode Phosphosilicate Optical Fibers for Radiation Detection," *IEEE Trans. Nucl. Sci.*, vol. 65, no. 1, pp. 126–131, Jan. 2018.
[132] B. D. Evans, G. H. Sigel, J. B. Langworthy, and B. J. Faraday, "The fiber optic dosimeter on the navigational technology satellite 2," *IEEE Trans. Nucl. Sci.*, vol. 25, no. 6, pp. 1619–1624, 1978.
[133] J. J. Suter, J. C. Poret, and M. Rosen, "Fiber optic ionizing radiation detector," *IEEE Trans. Nucl. Sci.*, vol. 39, no. 4, pp. 674–679, 1992.
[134] C. P. W. Boeder, L. Adams, and R. Nickson, "Scintillating fibre detector system for spacecraft component dosimetry," pp. 262–265, 2002.
[135] A. R. A. Rahim, N. A. Zahaimi, H. M. Zin, D. A. Bradley, G. A. Mahdiraji, and A. T. A. Rahman, "Characterisation of sensitive Ge-doped silica flat fibre-based thermoluminescence detectors for high resolution radiotherapy dosimetry," *J. Phys. Conf. Ser.*, vol. 851, pp. 1–6, May 2017.